Neurospheres From Human Adipose Tissue Transplanted Into Cultured Mouse Embryos can Contribute to Craniofacial Morphogenesis: A Preliminary Report

Takashi Nagase, MD, PhD,* Daisuke Matsumoto, MD,† Miki Nagase, MD, PhD,‡
Kotaro Yoshimura, MD, PhD,† Tomokuni Shigeura, MS,† Makoto Inoue, PhD,§
Mamoru Hasegawa, PhD,§ Masaaki Yamagishi, MD, PhD,* Masafumi Machida, MD, PhD*

Tokyo, Japan

Adipose-derived stromal cells (ASCs) are one of the most promising stem cell populations that differentiate into the mesodermal as well as neural lineages in vitro. In this study, we examined the neural differentiating potential of human ASCs by a neurosphere culture method. Neurospheres derived from human ASCs expressed *Nestin* and *Musashi-1* genes, which are marker genes for neural stem cells. When these cells were labeled with *green fluorescent protein* gene transfection by Sendai virus vector and transplanted into the head region of mouse embryos using a whole embryo culture system, these cells were incorporated into the craniofacial development. Some transplanted cells appeared to migrate along the second branchial arches, implicating some similarity to the cranial neural crest cells. Although preliminary, our results support an idea that ASC-derived neurospheres have properties of neural progenitors in vitro and in vivo.

From the *Clinical Research Center, National Hospital Organization Murayama Medical Center, Tokyo, Japan; †Department of Plastic and Reconstructive Surgery, ‡Department of Nephrology and Endocrinology, University of Tokyo Graduate School of Medicine, Tokyo, Japan; and §DNAVEC Corporation, Tsukuba, Ibaraki, Japan.

Address correspondence and reprint requests to Dr. Takashi Nagase, Head, Division of Advanced Medical Research, Clinical Research Center, National Hospital Organization Murayama Medical Center, 2-37-1 Gakuen, Musashimurayama-City, Tokyo 208-0011, Japan; E-mail: tnagase@fb3.so-net.ne.jp

The first two authors contributed equally to this work.

Key Words: Adipose-derived stromal cells, neurosphere, neural stem cells, embryo, stem cells

Adipose-derived stromal cells (ASCs) were originally reported as a subtype of the mesenchymal stem cells (MSCs) isolated from liposuction aspirates differentiating into the mesodermal tissues such as bone, cartilage, and adipose tissue.[1] Characterization of ASCs has recently been studied world wide by many groups, including ours.[2–4] ASCs are now regarded as one of the most promising adult stem cells for regenerative medicine because they can be harvested safely by liposuction, and a good yield can be anticipated.

Advances in stem cell research have resulted in a novel concept of cellular plasticity of differentiation beyond the boundary of germ layers. MSCs and ASCs can differentiate into neuronal (and thus ectodermal) derivatives, although these cells are primarily mesodermal.[5,6] Recent reports further indicate that stem cells with neural characteristics can be isolated from the mesodermal tissues such as the dermis and the heart.[7–9] In these cases, the cells were harvested by a neurosphere method, which was originally developed as a culture method of isolating spheres of neural stem cells from the embryonic and adult brain.[10–12] However, it is to be elucidated whether this method is also applicable for obtaining neural stem cells from the adipose tissue or ASCs.

In this study, the neurospheres expressing neural stem cell marker genes were obtained from human ASCs. We also transplanted these cells into mouse embryos cultured in vitro to examine whether these cells behave similar to neuronal cells in vivo.

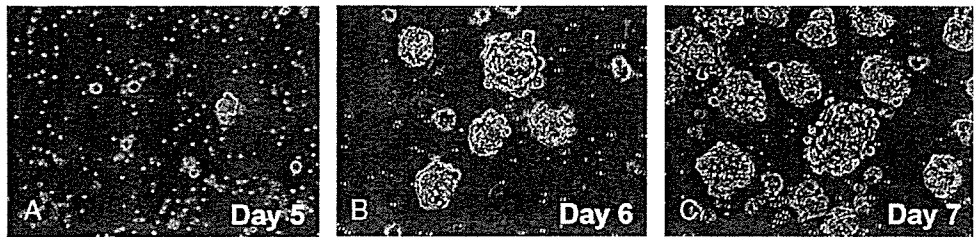

Fig 1 Neurosphere formation of adipose-derived stromal cells cultured in neurosphere medium for 5 days (A), 6 days (B), and 7 days (C) (magnification ×200).

MATERIALS AND METHODS

Isolation of Human ASCs and Neurosphere Cell Culture

ASCs were isolated from the human liposuction aspirates as reported previously.[3] The suctioned fat was digested with 0.075% collagenase in phosphate-buffered saline (PBS) for 30 minutes on a shaker at 37°C. Mature adipocytes and connective tissues were eliminated by centrifugation. Blood cells were also eliminated by treating with erythrocyte lysis buffer, and resultant ASC pellets were obtained. Alternatively, ASCs could be isolated from the fluid portions of liposuction aspirates by treating with erythrocyte lysis buffer and density gradient centrifugation with Ficoll (GE Healthcare Bio-sciences, Piscataway, NJ).

Neurosphere culture was performed as described previously with slight modification.[12] Freshly isolated ASCs were plated at a density of 2×10^7 cells in 10 cm uncoated dishes and cultured in the neurosphere culture medium at 37°C in an atmosphere of 5% CO_2 in humid air. The neurosphere medium was a Dulbecco's Modified Eagle's Medium/F12 (1:1)-based medium supplemented with human recombinant epidermal growth factor (EGF, 20 ng/mL, PeproTech, Rocky Hill, NJ), human recombinant basic fibroblast growth factor (FGF, 20 ng/mL, Kaken Pharmaceutical, Tokyo, Japan), 2% B27 supplement (Gibco, Carlsbad, CA), 100 U/mL penicillin, and 100 μg/mL streptomycin. Half of the medium was replaced with a fresh medium on the fourth to fifth day, and the passaging was performed on the eighth day.

Quantitative Real-Time Reverse-Transcriptase Polymerase Chain Reaction

Total mRNA was extracted using RNeasy-mini kit (Qiagen, Hilden, Germany) from the neurosphere cells derived from passage one ASCs, which were precultured in the normal medium containing M199 medium and 10% fetal bovine serum (FBS). The preculturing was necessary for reducing the contamination of blood cells. Control mRNA was also extracted from the passage one undifferentiated ASCs cultured in M199 plus 10% FBS.

Expressions of undifferentiated neural stem cell marker genes *Nestin* and *Musashi-1*[13] and adipogenic differentiation marker *Leptin* were analyzed by real-time quantitative reverse-transcription polymerase chain reaction (RT-PCR) using an ABI PRISM 7700

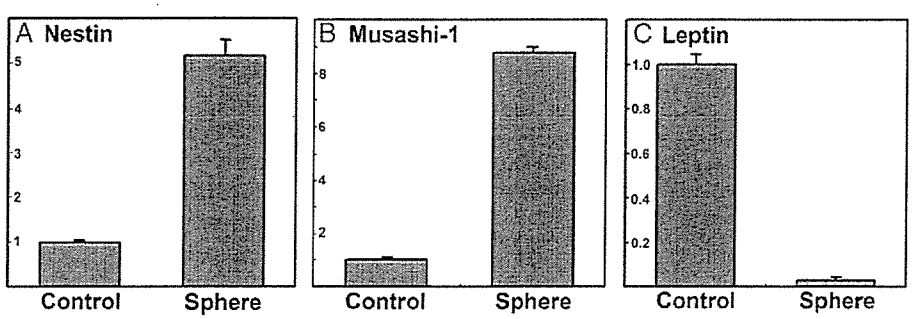

Fig 2 Quantitative real-time reverse-transcription polymerase chain reaction analysis of gene expressions of neural stem cell marker *Nestin* (A), *Musashi-1* (B), and adipogenic differentiation marker *Leptin* (C). Control = undifferentiated adipose-derived stromal cells; Sphere = neurospheres. Assays were performed in triplicate, and standard errors are indicated by error bars.

(Applied Biosystems, Foster City, CA), as reported previously. Gene expression of the target sequence was normalized to that of the housekeeping gene *β-actin.* Transcript level in the control (undifferentiated ASC) group was arbitrarily expressed as 1. TaqMan chemistry and assay by design primers and probe sets were used for human *Nestin, Musashi-1, Leptin,* and *β-actin.* All the primers and probe sets were purchased from Applied Biosystems.

Mouse Whole Embryo Culture and Transplantation of Neurosphere-Like Cells

Neurospheres derived from human ASCs were transfected with *green fluorescent protein* (*GFP*) gene using the Sendai virus vector (DNAVEC Corp. Tsukuba, Japan), as reported previously.[14,15] The original vector SeV/ΔF lacks the F gene encoding fusion protein necessary for penetration of ribonucleoprotein complex into infected cells, and is thus nontransmissible and nonpathogenic.[14] The modified SeV/ΔF vector has additional mutations to reduce its cytotoxicity,[15] and we used the modified vector in the present study. Neurospheres were incubated for 1 hour in the medium with the modified SeV/ΔF carrying the *GFP* gene at a multiplicity of infection of 250 and rinsed with PBS.

Mouse whole embryo culture was performed as reported previously.[16–19] Nine mouse embryos at embryonic day (E) 8 were dissected out without damaging yolk sacs, and the GFP-transfected neurosphere cells were transplanted using micropipettes into the head region of the embryos. The embryos were cultured for approximately 40 hours, and presence or absence of the GFP-positive transplanted cells was investigated under a fluorescent dissecting microscope. All experimental procedures were performed at the University of Tokyo under approval of the ethical committee.

RESULTS

We first cultured human ASCs in the neurosphere culture medium containing EGF and basic FGF without serum. On the third day of culture of freshly prepared ASCs, the floating ASCs started to form small masses (data not shown). The neurosphere-like cellular aggregates were clearly observed on the fifth day (Fig 1A). The number and the size of the spheres became increasingly larger within the next 2 days (Fig 1, B and C). The passaging was performed on the eighth day when the spheres were dissociated and resuspended in the new medium. The spheroids were newly formed after culturing again for several days (data not shown), suggesting self renewal of the neurosphere cells.

To characterize the neurosphere cells, we next examined expressions of neural stem cell marker *Nestin* and *Musashi-1* genes and adipocyte marker *Leptin* by quantitative real-time RT-PCR. Expressions of *Nestin* and *Musashi-1* genes were remarkably upregulated in the neurosphere cells compared with the control ASCs without culturing in the neurosphere medium (Fig 2, A and B), suggesting characteristics of neural progenitor. Conversely, *Leptin* expression

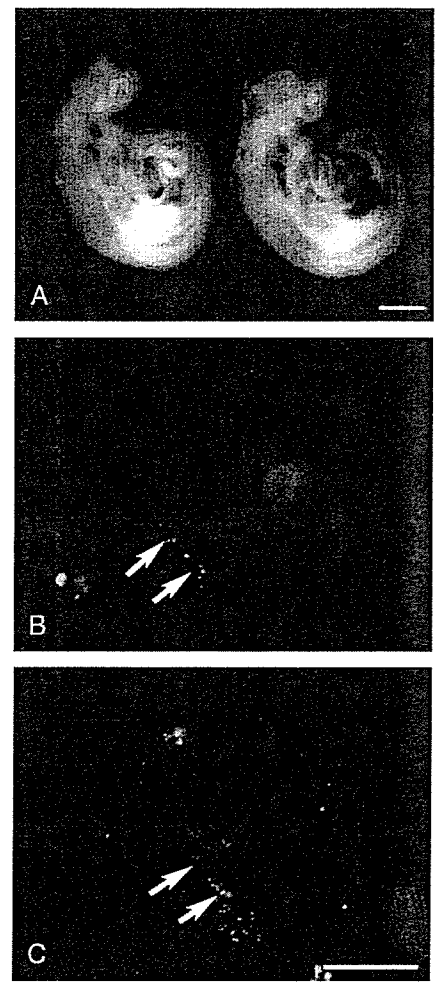

Fig 3 Neural crest-like migrations of green fluorescent protein (GFP)-transfected, adipose-derived stromal cell-derived neurospheres grafted into mouse embryo cultured in vitro. (A) Appearances of mouse embryos cultured for 40 hours from embryonic day 8. (B and C) Fluorescent views of embryos. GFP-positive neurosphere cells were arranged in a row (arrows), suggesting their migration along second branchial arch. Bars = 500 μm.

was dramatically reduced in the neurospheres (Fig 2C), indicating loss of adipogenic potential.

To investigate functions of the neurosphere cells in vivo, we labeled these cells by the modified Sendai virus vector carrying the *GFP* gene and transplanted them into the head region of the E8 mouse embryos. After the embryos were cultured for approximately 40 hours in vitro, the transplanted GFP-positive cells were clearly observed and appeared viable in only two embryos of the nine cultured embryos. The GFP-positive cells were incorporated into the craniofacial region as well as the heart and the trunk in these two embryos (Fig 3). Notably, the transplanted cells were arranged in a row along the second branchial arch (arrows in Fig 3, B and C) in a quite similar pattern to the neural crest cells migrating within the second branchial arch. Although not confirmatory, this result suggests a intriguing possibility that neurosphere cells derived from ASCs have neural crest-like properties.

Discussion

ASCs are probably one of the most well-known stem cells among plastic surgeons. ASCs were originally reported by Zuk et al[1] from the clinical samples of liposuction aspirates. According to their broad spectrum of differentiation potential, ASCs have been used in a number of preclinical animal studies of in vivo regeneration of a various tissues such as bone,[20,21] cartilage,[22] vessels,[4,23,24] soft tissue,[4] bone marrow,[25] and so on. Even a clinical case was reported, in which a calvarial defect was repaired by ASCs combined with scaffold.[26] Several groups reported neural differentiation of ASCs in vitro,[5,6,27] and Kang et al[28] reported functional recovery of the rat model with cerebral infarction after ASC transplantation in vivo.

The neurosphere method was originally reported by Reynolds et al[10,11] and is one of the most frequently used methods for isolating neural stem cells from the embryo or from the adult central nervous systems. However, this method has not yet been applied for obtaining neural stem cells from adipose tissue or the ASC population. In this preliminary study, we obtained neurospheres from the ASCs in human liposuction aspirates. Proliferation of these cells was quite rapid, possibly faster than other neurospheres from various tissue origins such as the dermis and the heart,[7–9] suggesting advantages of ASCs as a origin of neuronal progenitors for regenerative medicine. These neurosphere cells expressed *Nestin* and *Musashi-1*, marker genes for neural stem cells, probably reflecting their tendency of differentiating into neuronal progenitors. This view is further supported by inhibition of their expression of *Leptin*, a marker for adipogenic differentiation and maturation.

Do the ASC-derived neurosphere cells behave as neuronal progenitors in vivo? Our attempt of grafting these cells into the cultured mouse embryo revealed that some of the cells migrate along the second branchial arch and contribute to craniofacial morphogenesis. Their migratory pattern is quite similar to that of cranial neural crest cells, as we reported previously.[16] The neural crest cells are an embryonic cellular population characterized by extensive migration and a unique repertoire of differentiation.[29] The neural crest cells are often regarded as stem or progenitor cells for peripheral neurons and Schwann cells, and the craniofacial skeletal mesenchyme is also neural-crest derived.[17,19,29,30] Recent studies indicate that the neural crest stem cells can be harvested from the seemingly "mesodermal" tissues of adult animals, such as the dermis,[7] the hair follicular dermal papilla,[8] or the heart,[9] by means of the neurosphere method, implicating that it is also the case in the adipose tissue. Because our data are preliminary and we have a small sample size, further studies such as those with detailed expression analysis of neural/neural crest marker genes and large-scale in vivo grafting are necessary to confirm this interesting idea.

References

1. Zuk PA, Zhu M, Mizuno H, et al. Multilineage cells from human adipose tissue: implications for cell-based therapies. Tissue Eng 2001;7:211–228
2. Zuk PA, Zhu M, Ashjian P, et al. Human adipose tissue is a source of multipotent stem cells. Mol Biol Cell 2002;13: 4279–4295
3. Yoshimura K, Shigeura T, Matsumoto D, et al. Characterization of freshly isolated and cultured cells derived from the fatty and fluid portions of liposuction aspirates. J Cell Physiol 2006;208:64–76
4. Matsumoto D, Sato K, Gonda K, et al. Cell-assisted lipotransfer (CAL): supportive use of human adipose-derived cells for soft tissue augmentation with lipoinjection. Tissue Eng. In Press.
5. Ashjian PH, Elbarbary AS, Edmonds B, et al. In vitro differentiation of human processed lipoaspirate cells into early neural progenitors. Plast Reconstr Surg 2003;111:1922–1931
6. Kokai LE, Rubin JP, Marra KG. The potential of adipose-derived adult stem cells as a source of neuronal progenitor cells. Plast Reconstr Surg 2005;116:1453–1460
7. Toma JG, Akhavan M, Fernandes KJ, et al. Isolation of multipotent adult stem cells from the dermis of mammalian skin. Nat Cell Biol 2001;3:778–784
8. Fernandes KJ, McKenzie IA, Mill P, et al. A dermal niche for multipotent adult skin-derived precursor cells. Nat Cell Biol 2004;6:1082–1093
9. Tomita Y, Matsumura K, Wakamatsu Y, et al. Cardiac neural crest cells contribute to the dormant multipotent stem cell in the mammalian heart. J Cell Biol 2005;170:1135–1146
10. Reynolds BA, Tetzlaff W, Weiss S. A multipotent EGF-responsive

striatal embryonic progenitor cell produces neurons and astrocytes. J Neurosci 1992;12:4565–4574
11. Reynolds BA, Weiss S. Generation of neurons and astrocytes from isolated cells of the adult mammalian central nervous system. Science 1992;255:1707–1710
12. Kanemura Y, Mori H, Kobayashi S, et al. Evaluation of in vitro proliferative activity of human fetal neural stem/progenitor cells using indirect measurements of viable cells based on cellular metabolic activity. J Neurosci Res 2002;69:869–879
13. Kaneko Y, Sakakibara S, Imai T, et al. Musashi-1: an evolutionally conserved marker for CNS progenitor cells including neural stem cells. Dev Neurosci 2000;22:139–153
14. Li HO, Zhu YF, Asakawa M, et al. A cytoplasmic RNA vector derived from nontransmissible sendai virus with efficient gene transfer and expression. J Virol 2000;74:6564–6569
15. Inoue M, Tokusumi Y, Ban H, et al. Nontransmissible virus-like particle formation by F-deficient sendai virus is temperature sensitive and reduced by mutations in M and HN proteins. J Virol 2003;77:3238–3246
16. Nagase T, Sanai Y, Nakamura S, et al. Roles of HNK-1 carbohydrate epitope and its synthetic glucuronyltransferase genes on migration of rat neural crest cells. J Anat 2003;203: 77–88
17. Nagase T, Nagase M, Osumi N, et al. Craniofacial anomalies of the cultured mouse embryo induced by inhibition of sonic hedgehog signaling: an animal model of holoprosencephaly. J Craniofac Surg 2005;16:80–88
18. Nagase T, Nagase M, Yoshimura K, et al. Angiogenesis within the developing mouse neural tube is dependent on sonic hedgehog signaling: possible roles of motor neurons. Genes Cells 2005;10:595–604
19. Yamada Y, Nagase T, Nagase M, et al. Gene expression changes of sonic hedgehog signaling cascade in a mouse model of fetal alcohol syndrome. J Craniofac Surg 2005;16:1055–1061
20. Cowan CM, Shi YY, Aalami OO, et al. Adipose-derived adult stromal cells heal critical-size mouse calvarial defects. Nat Biotechnol 2004;22:560–567
21. Dragoo JL, Lieberman JR, Lee RS, et al. Tissue-engineered bone from bmp-2-transduced stem cells derived from human fat. Plast Reconstr Surg 2005;115:1665–1673
22. Dragoo JL, Samimi B, Zhu M, et al. Tissue-engineered cartilage and bone using stem cells from human infrapatellar fat pads. J Bone Joint Surg Br 2003;85:740–747
23. Planat-Benard V, Silvestre JS, Cousin B, et al. Plasticity of human adipose lineage cells toward endothelial cells: physiological and therapeutic perspectives. Circulation 2004;109: 656–663
24. Miranville A, Heeschen C, Sengenes C, et al. Improvement of postnatal neovascularization by human adipose tissue-derived stem cells. Circulation 2004;110:349–355
25. Cousin B, Andre M, Arnaud E, et al. Reconstitution of lethally irradiated mice by cells isolated from adipose tissue. Biochem Biophys Res Commun 2003;301:1016–1022
26. Lendeckel S, Jodicke A, Christophis P, et al. Autologous stem cells (adipose) and fibrin glue used to treat widespread traumatic calvarial defects: case report. J Craniomaxillofac Surg 2004;32:370–373
27. Fujimura J, Ogawa R, Mizuno H, et al. Neural differentiation of adipose-derived stem cells isolated from GFP transgenic mice. Biochem Biophys Res Commun 2005;333:116–121
28. Kang SK, Lee DH, Bae YC, et al. Improvement of neurological deficits by intracerebral transplantation of human adipose tissue-derived stromal cells after cerebral ischemia in rats. Exp Neurol 2003;183:355–366
29. Le Douarin N, Kalcheim C. *The Neural Crest*, ed 2. Cambridge: Cambridge University Press, 1999
30. Nagase T, Nakamura S, Harii K, et al. Ectopically localized HNK-1 epitope perturbs migration of the midbrain neural crest cells in pax6 mutant rat. Dev Growth Differ 2001;43: 683–692

Induction of Efficient Antitumor Immunity Using Dendritic Cells Activated by Recombinant Sendai Virus and Its Modulation by Exogenous *IFN-β* Gene[1]

Satoko Shibata,*† Shinji Okano,* Yoshikazu Yonemitsu,[2]* Mitsuho Onimaru,* Shihoko Sata,* Hiroko Nagata-Takeshita,* Makoto Inoue,‡ Tsugumine Zhu,‡ Mamoru Hasegawa,‡ Yoichi Moroi,† Masutaka Furue,† and Katsuo Sueishi*

Dendritic cell (DC)-based cancer immunotherapy has been paid much attention as a new and cancer cell-specific therapeutic in the last decade; however, little clinical outcome has been reported. Current limitations of DC-based cancer immunotherapy include sparse information about which DC phenotype should be administered. We here report a unique, representative, and powerful method to activate DCs, namely recombinant Sendai virus-modified DCs (SeV/DC), for cancer immunotherapy. In vitro treatment of SeV without any bioactive gene solely led DCs to a mature phenotype. Even though the expression of surface markers for DC activation ex vivo did not always reach the level attained by an optimized amount of LPS, superior antitumor effects to B16F1 melanoma, namely tumor elimination and survival, were obtained with use of SeV-GFP/DC as compared with those seen with LPS/DC in vivo, and the effect was enhanced by SeV/DC-expressing IFN-β (SeV-murine IFN-β (mIFN-β)/DC). In case of the treatment of an established tumor of B16F10 (7–9 mm in diameter), a highly malignant subline of B16 melanoma, SeV-modified DCs (both SeV-GFP/DC and SeV-mIFN-β/DC), but not immature DC and LPS/DC, dramatically improved the survival of animals. Furthermore, SeV-mIFN-β/DC but not other DCs could lead B16F10 tumor to the dormancy, associated with strongly enhanced $CD8^+$ CTL responses. These results indicate that rSeV is a new and powerful tool as an immune booster for DC-based cancer immunotherapy that can be significantly modified by IFN-β, and SeV/DC, therefore, warrants further investigation as a promising alternative for cancer immunotherapy. ***The Journal of Immunology,*** **2006, 177: 3564–3576.**

Cancer vaccines have focused on the induction of CTLs that specifically attack tumor cells in an Ag-restricted manner without exerting a significantly harmful effect on nontumor cells. The induction of tumor-specific $CD4^+$ T cells is also important not only in helping the $CD8^+$ CTL response but also in mediating antitumor effector functions through the induction of eosinophils and macrophages (1). To boost these immune responses, several substances have been used as cancer vaccines, including gene-modified autologous tumor cells, peptide vaccine, plasmid DNA, and Ag-loaded dendritic cells (DCs)[3] (2). Despite current extensive efforts by physicians and scientists in clinical studies of cancer immunotherapy, very little clinical outcome has been reported (3).

DCs are the most potent and professional APCs that determine either Th1 or Th2 polarization of naive T cells, and they have been a promising tool for cancer immunotherapy. The immature state of DCs is known to be appropriate for Ag processing, and in turn, they must be matured to fully activated DCs, which express high levels of cell surface MHC-Ag complex and costimulatory molecules, for a sufficiently productive CTL response (4). Since the first promising clinical study of a DC-based cancer vaccine was reported in 1996 (5), similar studies have been performed using this type of vaccine against several cancers, including metastatic melanoma, all over the world (6–7). These early clinical trials suggested the potential of DC-based immunotherapy, but the extensive follow-up studies concluded that the current strategy remains immature as a standard therapeutic for cancer treatment (2).

Current issues of DC-based cancer immunotherapy include a lack of information regarding the following points: 1) the most effective DC subtypes, 2) the optimal conditions and activation stimuli to generate activated DCs showing optimal antitumor effect in vivo, 3) the optimal route for administration, and 4) the optimal dose and frequency of DC vaccinations (2). Because no one knows what the optimal performance and precise clinical indications of DC-based cancer immunotherapy are at present, preclinical assessment regarding these points in detail is absolutely required to obtain more data about DC therapy in clinical settings.

Currently, "virotherapy" is an indicative term for tumor-selective oncolytic virus therapy for cancer, namely "oncolytic virotherapy" (8). However, the first use of the term virotherapy appeared in a Japanese article in 1960, demonstrating the modest antitumor effect of a direct intratumor (i.t.) and/or intradermal injection of bovine vaccinia virus for patients with skin cancers (9).

*Division of Pathophysiological and Experimental Pathology, Department of Pathology and †Department of Dermatology, Graduate School of Medical Sciences, Kyushu University, Fukuoka, Japan; and ‡DNAVEC Corporation, Tsukuba, Ibaraki, Japan

Received for publication August 11, 2005. Accepted for publication June 23, 2006.

The costs of publication of this article were defrayed in part by the payment of page charges. This article must therefore be hereby marked *advertisement* in accordance with 18 U.S.C. Section 1734 solely to indicate this fact.

[1] This work was supported in part by a Grant-in-Aid (to Y.Y. and K.S.) from the Japanese Ministry of Education, Culture, Sports, Science, and Technology; and by the Program for Promotion of Fundamental Studies in Health Sciences of the National Institute of Biomedical Innovation (to Y.Y. and K.S.; Project MF-21).

[2] Address correspondence and reprint requests to Dr. Yoshikazu Yonemitsu, Division of Pathophysiological and Experimental Pathology, Department of Pathology, Graduate School of Medical Sciences, Kyushu University, 3-1-1 Maidashi, Higashi-ku, Fukuoka 812-8582, Japan. E-mail address: yonemitu@med.kyushu-u.ac.jp

[3] Abbreviations used in this paper: DC, dendritic cell; SeV, recombinant Sendai virus; SeV/DC, SeV-modified DC; mIFN-β, murine IFN-β; mBM-DC, bone marrow-derived DC; i.t., intratumoral; T-reg, regulatory T; MOI, multiplicity of infection; LCMV, lymphocytic choriomeningitis virus; fsc/ssc, forward scatter/side scatter.

0022-1767/06/$02.00

This use of the term virotherapy, therefore, included the concept of "immunostimulatory virotherapy."

In the last decade, we extensively examined the use of recombinant Sendai virus (SeV) as a novel and powerful gene transfer agent as the cytoplasmic gene expression system (10–12). SeV, a member of family *Paramyxoviridae*, has a nonsegmented negative-strand RNA genome and makes use of sialic acid residue on surface glycoprotein or asialoglycoprotein present on most cell types as a receptor (13, 14). As SeV uses a cytoplasmic transcription system, it can mediate gene transfer to a cytoplasmic location, avoiding possible malignant transformation due to genetic alteration of host cells (10, 15), that is a safety advantage of SeV. Furthermore, there are technical advantages in the use of rSeV as a gene therapy vector; first, the infectious activity of SeV particles is stable to be easily concentrated to high titers by ultracentrifugation, which is in clear contrast to the features of retroviral vectors. Second, and most importantly, the modalities of target cell processing and viral transduction are technically nondemanding and feasible in clinical situations that require transduction into large numbers of target cells, including hemopoietic stem cells (16). Despite these advantageous features of SeV in clinical gene therapy strategies over the other vector systems (10–12), the related immune responses due to virus administration in vivo have been hazardous to expand the use of this mode of vector in the clinical setting, similar to other viral vectors including adenoviruses. During extensive assessment of the mechanisms of immune responses against SeV, we found that ex vivo infection of SeV to immature DCs resulted in their maturation and activation spontaneously, suggesting their possible use for cancer immunotherapy as an immunostimulatory virotherapy.

In the present study, for the first time, we show that i.t. administration of replication-competent SeV-modified DCs (SeV/DCs) induces a dramatically efficient antitumor effect on established tumors in vivo, an effect comparable to that seen with DCs treated with LPS that is well-known as a strong DC stimulator irrelevant to clinical use. Furthermore, we here show that antitumor immunity against an IFN-β-sensitive tumor, a B16 melanoma, is strongly enhanced by the use of SeV/DCs expressing a foreign *IFN-β* gene.

Materials and Methods

Mice and tumor cell lines

Female 6- to 8-wk-old C57BL/6 mice (H-2^b, for B16 melanomas) and C3H/HeN mice (H-2^k, for MH134) of Charles River grade were obtained from KBT Orientals and kept under specific pathogen-free and humane conditions. Murine malignant melanoma B16F1 and B16F10 cells were purchased from American Culture Collections (ATCC). MH134, a murine hepatocellular carcinoma cell line, and X5563, a plasmacytoma cell line derived from C3H/HeN mice, were maintained as described (17). An NK-sensitive lymphoma cell line, YAC-1, and a T cell lymphoma cell line of C57BL/6 mice origin, EL-4, were also purchased from ATCC. These cell lines were maintained in complete medium (RPMI 1640 medium; Sigma-Aldrich) supplemented with 10% FCS (BioWest), penicillin, and streptomycin under a humidified atmosphere containing 5% CO_2 at 37°C.

Recombinant SeVs

rSeVs were constructed as described previously (10). In brief, the entire cDNA-coding jelly fish enhanced GFP (for SeV-GFP), luciferase (for SeV-luciferase), and murine IFN-β (for SeV-mIFN-β) were amplified by PCR, using primers with a *NotI* site and new sets of SeV E and S signal sequence tags for an exogenous gene, and then inserted into the *NotI* site of the cloned genome. Template SeV genomes with an exogenous gene and plasmids encoding N, P, and L proteins (plasmids pGEM-N, pGEM-P, and pGEM-L, respectively) were conjugated with commercially available cationic lipids, then cotransfected with UV-inactivated vaccinia virus vT7–3 into LLMCK2 cells. Forty hours later, the cells were disrupted by three cycles of freezing and thawing and injected into the chorioallantoic cavity of 10-day-old embryonated chicken eggs. Subsequently, the virus was recovered and the vaccinia virus was eliminated by a second propagation in eggs. Virus titer was determined using chicken RBC in a hemagglutination assay, and viruses were kept frozen at −80°C until use. Expression of mIFN-β was confirmed by Western blotting in the culture medium of COS7 cells and DCs transfected with SeV-mIFN-β (data not shown).

Generation of DCs and transfection with SeVs

When preparing murine bone marrow-derived DCs (mBM-DCs), we paid serious attention to maintaining an endotoxin-free condition using endotoxin-free reagents throughout this study. mBM-DCs were generated as previously described with minor modification (18, 19). Briefly, bone marrow cells from C57BL/6 or C3H/HeN mice were collected and passed through a nylon mesh, and RBC and lineage-positive (B220, CD5, CD11b, Gr-1, TER119, 7/4) cells were depleted by using the SpinSep mouse hemopoietic progenitor enrichment kit (StemCell Technologies). These lineage-negative cells (5–10 × 10^4/5 ml/well) were cultured in 50 ng/ml GM-CSF (PeproTech) and 25 ng/ml IL-4 (PeproTech) in endotoxin-free complete medium in 6-well plates. On day 4, half of the culture medium was replaced by fresh medium supplemented with GM-CSF and IL-4 at the same concentration. On day 7, DCs were collected and used for subsequent experiments. For SeV-mediated transduction, DCs (1 × 10^6 cells/ml) were simply incubated with SeVs at an indicated multiplicity of infection (MOI) without any supplementation.

In vitro cytotoxic assay with IFN-β

B16F1, B16F10, and MH134 cells were seeded in 96-well plates at 5000 cells/well, and 24 h later, recombinant murine IFN-β (rmIFN-β; PBL Biomedical Laboratories) was added to each well at various concentrations. Forty-eight hours later, cell viability was assessed by a modified MTT assay using a Cell Counting Kit-8 (Dojin Laboratories). Results were calculated as the percentage of viability = (OD of sample − OD of blank)/(OD of A − OD of blank) × 100, where OD corresponds to A wells without rmIFN-β.

Influence of MHC class I expression on tumor cells by IFN-β

B16F1, B16F10, and MH134 cells (1 × 10^5/ml) were incubated in the presence or absence of rmIFN-β (1000 U/ml) at 37°C for 48 h. B16 or MH134 cells were collected and stained with FITC-conjugated anti-mouse H-$2K^b$ or H-$2K^k$ (BD Pharmingen), respectively, and were analyzed using a FACSCalibur (BD Biosciences). Dead cells were excluded by staining with propidium iodide.

Luciferase assay

The collected mBM-DCs were treated with lysis buffer (Promega) with a protease inhibitor mixture (10), centrifuged, and 20 μl of the supernatant was subjected to luciferase assay. Light intensity was measured after 10 s of preincubation at room temperature using a luminometer (model LB9507; EG&G Berthold) with 10 s integration. Protein concentrations were measured by Bradford's method using a commercially available protein assay system (Bio-Rad) (11). The data were expressed as relative light units per milligram of protein, and each sample was measured more than twice.

Flow cytometric analysis for costimulation-related molecules on DCs

DCs were plated in fresh medium (1 × 10^6 cells/ml) and were incubated with SeV-GFP or SeV-mIFN-β, each at a MOI of 40, or LPS (2 μg/L) for 48 h. Biotinylated anti-mouse I-Ab, CD40, CD80, CD86, CCR7, ICAM-1, and allophycocyanin-conjugated anti-CD11c (BD Pharmingen) mAbs were used for each primary Ab. The collected DCs were centrifuged and incubated with 100 μl of the supernatant from cultured hybridoma-producing anti-mouse CD16/32 mAb (2.4G2; from ATCC) for 30 min at 4°C. The cells were incubated with primary Abs for 30 min at 4°C, and biotinylated Abs were detected by subsequent staining with streptavidin-PE (BD Pharmingen). Just before application to the cytometer, we added 125 ng of propidium iodide to cell suspension to exclude dead cells. Cells were analyzed using a FACSCalibur with the CellQuest software (BD Biosciences Japan). Data analysis was performed using FlowJo 4.5 software (Tree Star).

Cytokine production of cultured DCs

The cultured DCs were plated in fresh medium (1 × 10^6 cells/ml) and were incubated with SeV-GFP or SeV-mIFN-β (MOI of 40) or LPS (2 μg/l) for 48 h. The culture medium were harvested and were measured the concentration of murine IFN-β, IFN-γ, IL-12 p70, TNF-α, and IL-1β by quantitative sandwich enzyme immunosorbent assay using mouse IFN-β, IFN-γ,

IL-12 p70, TNF-α, and IL-1β ELISA kit (R&D Systems) according to the manufacturer's instructions.

DC-based immunotherapy of the established tumor

B16F1 melanoma: early treatment regimen (see Fig. 2). For tumor lysate preparation, B16 melanoma cells were harvested and processed by three rapid cycles of freezing and thawing. As a control, mBM-DCs with neither tumor lysate nor stimulator were used. The other mBM-DCs were pulsed with tumor lysate (ratio of DC number to number of tumor cells for lysate = 1:3) for 18 h and then were incubated with SeV-GFP (MOI = 40; SeV-GFP/DCs), SeV-mIFN-β (MOI = 40; SeV-mIFN-β/DCs), or LPS (2 μg/L; LPS/DCs) for 8 h. Then all DCs were added with 50 μg/ml polymyxin B (Sigma-Aldrich) and were carefully washed two times before injection. Intradermal implantation (C57BL/6 for 1×10^5 B16F1 cells) was done onto the abdomen on day 0, and 1×10^6 DCs were injected i.t. on days 3, 10, and 17. For all injections, materials were suspended in a 100-μl volume of PBS. The size of tumors was assessed using microcalipers three times a week, and the volume was calculated by the following formula: (tumor volume; mm^3) = 0.5236 $\times$ (long axis) $\times$ (short axis) $\times$ (height) (20).

B16F10 melanoma and MH134 hepatocellular carcinoma: later treatment regimen (see Fig. 4). To examine the potentials of cancer vaccines tested here to treat highly malignant phenotypes in vivo, we further assessed "later treatment regimen" when the tumors were well-established and vascularized (7–9 mm in diameter) (3).

DCs were collected as described above, except for control DCs which were pulsed with tumor lysate but not stimulated. Intradermal implantation (C57BL/6 for 1×10^5 B16F10 cells and C3H/HeN for 1×10^6 MH134 cells) was done onto the abdomen on day 0, and 1×10^6 DCs were injected i.t. on days 10, 17, and 24. The size of tumors was assessed as described above.

^{51}Cr release assay for cytolytic activity of NK cells and CTLs

Prepared DCs were i.t. administered three times into tumor-bearing C57BL/6 mice (B16F10) or C3H/HeN mice (MH134) at 1×10^6 cells/100 μl on days 10, 17, and 24. One week after the last immunization, splenocytes were obtained and contaminated erythrocytes were depleted by 0.83% ammonium chloride. For NK cell-lysis assay, the splenocytes were directly used as NK effector cells. For CTL assay, 4×10^6 splenocytes were cultured with 1 μM TRP-2 peptide ($H\text{-}2^b$-restricted peptide = SVYDFFVWL) (21) for B16 melanoma model, or with 3×10^5 inactivated MH134 cells treated with 100 μg/ml mitomycin for the MH134 model in 1 ml of complete medium in a 24-well culture plate. Two days later, 30 IU/ml human rIL-2 was added to the medium. After 5 days, the cultured cells were collected and used as CTL effector cells. Target cells (YAC-1, TRP2-peptide-pulsed EL-4, lymphocytic choriomeningitis virus (LCMV) peptide (H-2b-restricted peptide = AVYNFATCGI) pulsed EL-4 (for third party of B16), MH134 cells, and X5633 (for third party of MH134)) were labeled with 100 μCi $Na_2{}^{51}CrO_4$ for 1.5 h, and Cr release assay was performed as previously described (22). The percentage of specific ^{51}Cr release of triplicates was calculated as follows: ((experimental cpm − spontaneous cpm)/(maximum cpm − spontaneous cpm)) $\times$ 100. Spontaneous release was always <10% of maximal Cr release (target cells in 1% Triton X-100).

In vivo depletion of immune cell subsets

Anti-CD4 and anti-CD8 mAbs (250 μg/dose) were derived from GK1.5 and 53-6.72 hybridoma cells, respectively (23, 24). Anti-asialo GM1 (Wako) was given i.p. (50 μg/dose) for NK cell depletion. Elimination of $CD4^+$ or $CD8^+$ cells in tumor-bearing mice (n = 4–5 in each group) was done by i.p. injection of mAbs on days 5, 6, 7, 10, 13, 16, 19, 21, 24, 27, and 30 after the primary tumor inoculation. Flow cytometry confirmed >98% depletion of the target cells for at least 7 days after injection in all animals.

Histopathological analysis

B16F10 tumor was treated twice (days 10 and 17), and freshly excised tumor tissues on day 20 were divided into the longitudinal two sections; the half was embedded in Tissue-Tec OCT compound (Sakura) and the other was embedded in paraffin. Paraffin sections were stained with H&E. The cryostat sections were subjected to immunochemical examinations with mAbs specific to CD4 (L3T4; BD Pharmingen) or CD8 (Ly-2; BD Pharmingen). Tumor area was measured by Macscope (Mitani). CD4- or CD8-positive cells were counted in total viable tumor area and peripheral stromal tissue within 0.5 mm from the margins of tumor tissue under the optical measure-assisted microscope.

Statistical analysis

All data were expressed as the mean ± SEM, and were analyzed by one-way ANOVA with Fisher's adjustment, except for animal survival. Survival was plotted using Kaplan-Meier curves and statistical relevance was determined using log-rank comparison. A probability value of $p < 0.05$ was considered significant.

Results

Transfection efficiency of SeV into mBM-DCs and their spontaneous activation

Immature mBM-DCs from BL/6 mice, propagated in the presence of GM-CSF and IL-4 for 7 days, were collected and transfected by SeV-luciferase or SeV-GFP for investigating gene transduction efficiency. As shown in Fig. 1*a*, *left panel*, dose-dependent luciferase expression was shown and the optimized expression was found around MOI = 40–100. Repeated FACS analyses for DCs transfected by SeV-GFP demonstrated that >90% of GFP-positive DCs were detected at more than MOI = 40, a finding representatively shown with forward scatter/side scatter (fsc/ssc) gating at MOI = 40 (Fig. 1*b*), therefore, all of the following experiments were performed at this titer as an optimal dose.

We next assessed the surface markers of DCs treated with SeV-expressing GFP or mIFN-β without any other stimulant, directly compared with a well-known strong but clinically irrelevant DC activator, LPS, at 2 μg/ml for 48 h of exposure, which had been shown to be the optimal dose for mDC activation in our preliminary data (data not shown). As shown in Fig. 1*c*, repeated FACS analyses showed that DCs treated with SeV-GFP or SeV-mIFN-β resulted in the high-level expression of the costimulatory molecules tested here, namely MHC class II, CD80, and CD86 molecules, which did not reach the level seen in the DCs treated with LPS. In comparison to their sharp expression patterns on LPS/DC, those seen on SeV-GFP or SeV-mIFN-β showed broad expression, suggesting the result of the broad expression of transgene seen in Fig. 1*b*. Other surface markers related to trafficking (CCR7) and adhesion (ICAM-1) were also up-regulated on DCs treated with SeV-GFP or SeV-mIFN-β which were nearly comparable to the level seen on LPS/DC. These results thus demonstrated that SeV could not only effectively transfer exogenous genes into DCs, but also spontaneously transform immature DCs to near fully activated mature DCs without other manipulation irrespective of the exogenous mIFN-β expression. In turn, LPS-activated DCs were seriously resistant to SeV-mediated gene transfer (usually <5%, data not shown).

To assess further phenotype of DCs activated by SeV, release of typical cytokines was examined by ELISA. As shown in Fig. 1*d*, up-regulation of type I IFN, e.g., IFN-β, was seen in DCs treated with SeV-GFP or SeV-mIFN-β, but not in immature DCs and LPS/DCs. In contrast, strongest expression of other cytokines tested, including Th1 cytokines (p70 subunit of IL-12 and IFN-γ), was seen in LPS/DCs.

Together with these results, SeV induces spontaneous maturation and activation of mBM-DCs, however, their phenotype is not equal to those seen in the treatment with LPS.

SeV/DC therapy induces complete elimination of B16F1 melanoma in vivo

Next, we asked whether DCs activated by SeV might have therapeutic potentials against an immune-competent murine melanoma model. We tested this by an early treatment regimen as follows.

First, to assess the effective route for antitumor activity of DC therapy, i.t., distant s.c., and i.v. (via tail vein, i.v.) injections of tumor lysate-pulsed DCs activated by SeV-GFP was started and

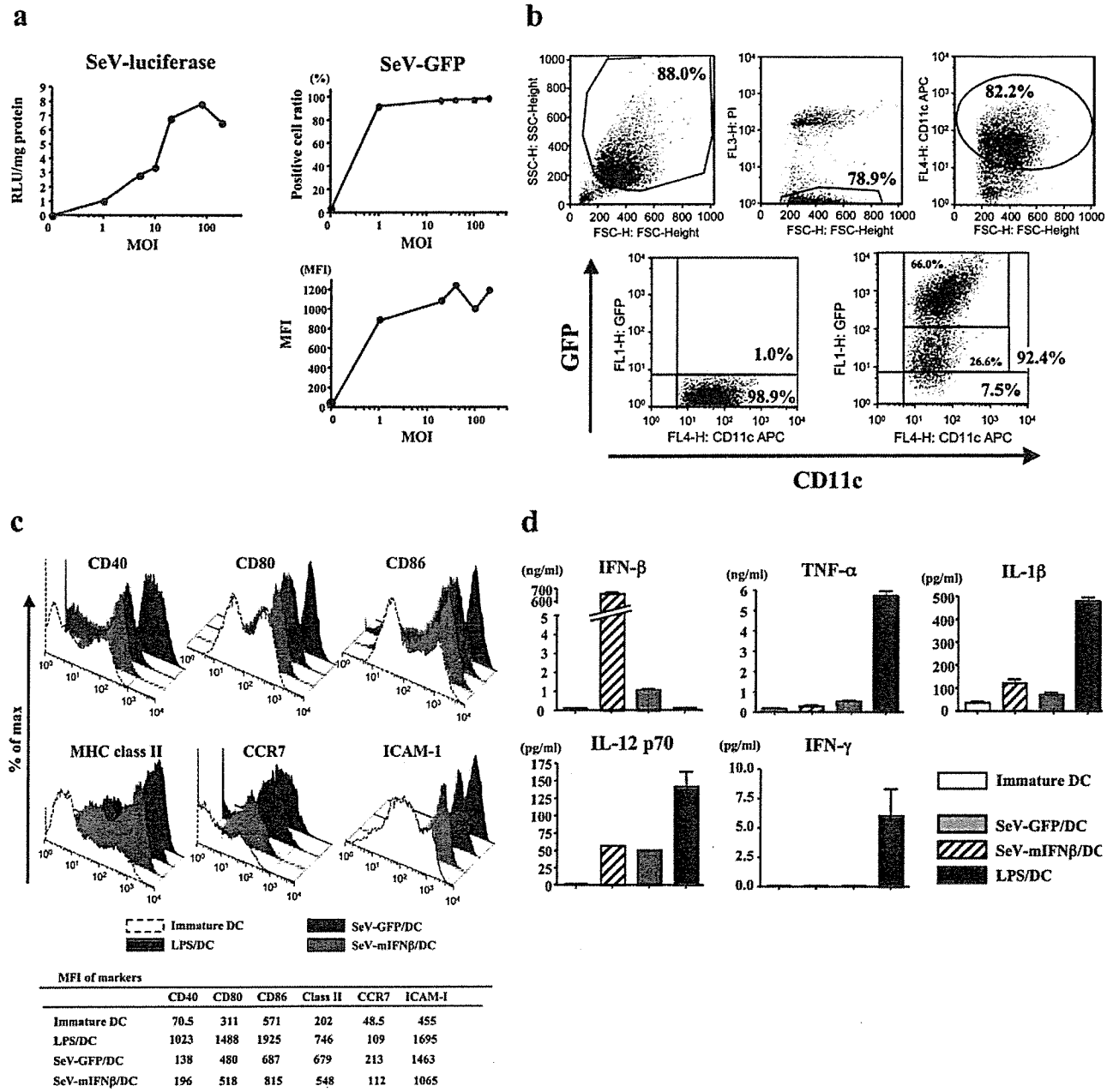

MFI of markers

	CD40	CD80	CD86	Class II	CCR7	ICAM-I
Immature DC	70.5	311	571	202	48.5	455
LPS/DC	1023	1488	1925	746	109	1695
SeV-GFP/DC	138	480	687	679	213	1463
SeV-mIFNβ/DC	196	518	815	548	112	1065

FIGURE 1. Gene transfer efficiency of SeV to bone marrow-derived immature DCs and their spontaneous activation. Seven days after cultivation to generate immature DCs under IL-4 and GM-CSF, DCs were treated by SeV-luciferase or SeV-GFP. Forty-eight hours later, DCs were subjected to each analysis. Each experiment was done in triplicate or more and showed similar results. *a*, Quantitative optimization of dose-dependent gene expression efficiency using SeV-luciferase (*left graph*) and SeV-GFP (*upper right two graphs*: positive cell ratio, *bottom*: MFI, mean fluorescent intensity). Optimized expression was seen around MOI = 40–100. *b*, Scattered plots for fsc/ssc gating of DCs transfected with SeV-GFP at MOI = 40. Note 2 major populations of GFP-expressing DCs, GFP^{high} (66.0%) and GFP^{low} (26.6%) (*bottom right panel*). *c*, Expression level of activation markers (CD40, CD80, CD86, MHC class II) and Ags related to trafficking (CCR7) and to adhesion (ICAM-1) of DCs, treated with SeV-GFP, SeV-mIFN-β, or LPS (2 μg/ml). MFIs of each analysis were given below. *d*, Typical cytokine secretion from DCs treated with LPS, SeV-GFP, or SeV-mIFN-β. Immature DCs were used as negative control.

repeated three times every week 3 days after B16F1 (low malignant subline) cell inoculation. Efficient antitumor effect was only seen in the case of i.t. injection (Fig. 2*a*), a finding similar to the previous report by the other group in use of naive DCs (25). Therefore, the following experiments were done via the i.t. route.

Next, we directly compared the antitumor effect of i.t. administration of immature DC, LPS/DC/lysate, SeV-GFP/DC/lysate, and SeV-mIFN-β/DC/lysate by early treatment regimen indicated in Fig. 2*b*. In this study, we used immature DCs without tumor lysate as a control, because it has been known that ex vivo uptake of tumor Ag itself led DCs to activated state (26). Because B16 melanoma-burden mice were well-known to start to die around 2 wk after inoculation irrespective of tumor size, we here evaluated two more parameters, namely survival and the number of mice with eliminated tumor, to assess the beneficial effects of cancer vaccines.

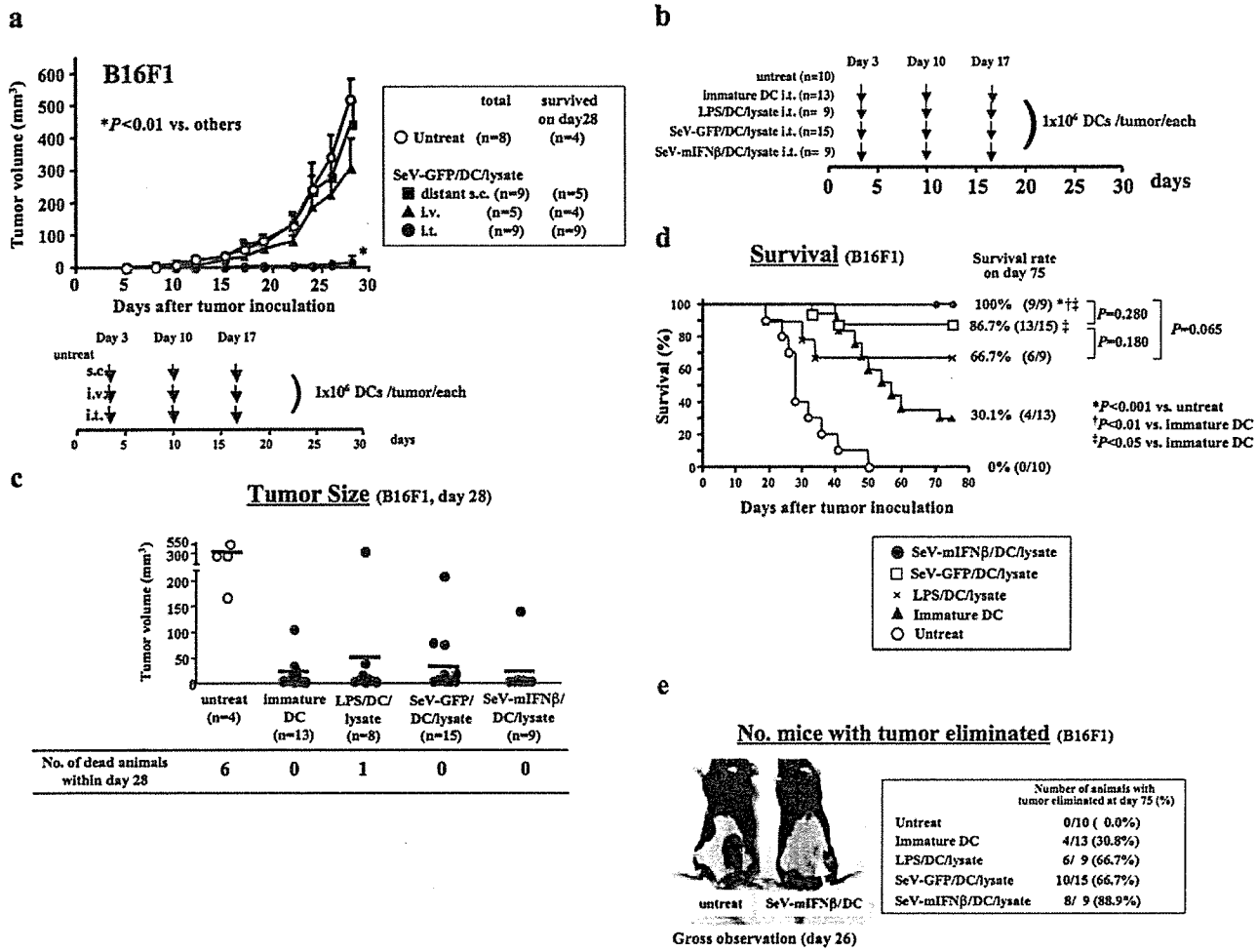

FIGURE 2. Assessment of antitumor activity of DCs modified by SeV against low-malignant murine melanoma B16F1. Three days after tumor cell inoculation, DCs were injected i.t. according to the indicated regimen (*a*, *bottom scheme*: early treatment regimen). Tumor lysate was pulsed to immature DCs which were subsequently treated with LPS, SeV-GFP, or SeV-mIFN-β, and these DCs were used for DC immunotherapy 8 h later. DC treatment was done three times. The data demonstrated were the total of three independent experiments. *a*, Time course of the tumor volume treated with SeV-GFP/DC/lysate via different administration routes (distant s.c.: s.c. injection, i.v.: i.v. injection via tail vein, and i.t.: intratumor injection). Numbers indicate tumor-bearing animals that survived over 28 days. *b*, Experimental design to assess the stimulator dependent antitumor effect of DCs. *c*, Dot plots indicating the tumor size of B16F1 melanoma following DC therapy. Numbers below indicate the dead animals within day 28. *d*, Survival curve of the mice bearing B16F1 melanoma treated with various DCs. Significant prolongation of survival was seen in SeV/DC groups. *e*, Typical and representative gross observation of mice with B16F1 tumors treated with or without SeV-mIFN-β/DC/lysate 26 days after tumor cell inoculation. Note complete rejection of tumors by SeV-mIFN-β/DC/lysate treatment (arrow), which was confirmed by histopathological examination (data not shown). Tumor rejection rate of mice at day 75 was also presented in the right column.

Tumor size. As shown in Fig. 2*c*, six animals of the untreated group and 1 of the LPS/DC/lysate group were dead within day 28. The tumor size on day 28 was efficiently disturbed by DC immunotherapy modified by SeV-GFP, SeV-mIFN-β, or LPS. However, a similar finding was also seen in the use of immature DCs, suggesting the results of spontaneous activation of DCs in vivo via i.t. route, as previously described by the other group (25).

In contrast, other parameters, survival, and tumor elimination ratio showed interesting results.

Survival. Significant prolongation of survival of animals was found only in groups of SeV-GFP/DC/lysate and SeV-mIFN-β/DC/lysate (Fig. 2*d*).

Number of mice with tumor eliminated. Ten of 14 mice (71.4%) treated with SeV-GFP/DC and 8 of 9 (88.9%) treated with SeV-mIFN-β/DC completely eliminated the tumor at day 75 (Fig. 2*e*), findings that were also confirmed microscopically (data not shown).

These results indicated that DC immunotherapy was beneficial for treating B16F1 melanoma in immune-competent mice, in views of survival and tumor elimination, and the therapeutic effects of DCs modified with SeV were equal or possibly more to that with strong DC activator LPS, an effect that was significantly improved by exogenous IFN-β expression.

Limited responses of mIFN-β protein as well as mIFN-β gene therapies on highly malignant and less immunogenic B16F10 melanoma in vivo

Direct efficacy evaluation demonstrated in Fig. 2 suggests the potential use of SeV-mediated modification of DC functions for cancer immunotherapy; however, significant and clear improvement over LPS/DC was not found. Furthermore, immature DCs showed significant reduction of tumor size, suggesting that the tumor model of low malignant B16F1 melanoma was not appropriate to evaluate the potentials of SeV/DCs. Therefore, we next tried to

treat a highly malignant and less immunogenic subtype of B16 melanoma, namely B16F10, using SeV/DCs. Before this trial, we first assessed the biological effects of mIFN-β in vitro and of protein and gene therapy with mIFN-β in vivo.

As shown in Fig. 3*a*, mild and dose-dependent growth inhibition was seen in B16F1 cells in vitro, and the effect was more pronounced in B16F10 cells, indicating that B16 melanomas are sensitive to IFN-β, similar to findings in clinical settings (27). In contrast, murine hepatocellular carcinoma, MH134, was not apparently sensitive to IFN-β (Fig. 3*a*).

Next, we treated B16F10 tumors in vivo with mIFN-β protein, which has been a standard clinical therapeutic, as well as with SeV-mIFNβ as a gene therapy, by a treatment regimen beginning at a later stage of tumor development (tumor diameter = 7–9 mm). As shown in Fig. 3*b*, both treatments tended to delay the growth of the B16F10 tumors; however, the tumor volume had relapsed by about day 30. The relapse of tumor growth was likely due to withdrawal of the local concentration of mIFN-β, because in vivo expression of SeV-mediated gene transfer has been shown to be transient (11).

These findings suggest that protein and gene therapies by mIFN-β contributed to the suppression of tumor growth of B16F10 tumors in vitro and in vivo; however, the effect was not sufficient to control a highly malignant cell type, even though the tumor cells are sensitive to mIFN-β. This could be explained because the duration of local concentration of mIFN-β might not be sufficient to show the long-lasting antitumor effect.

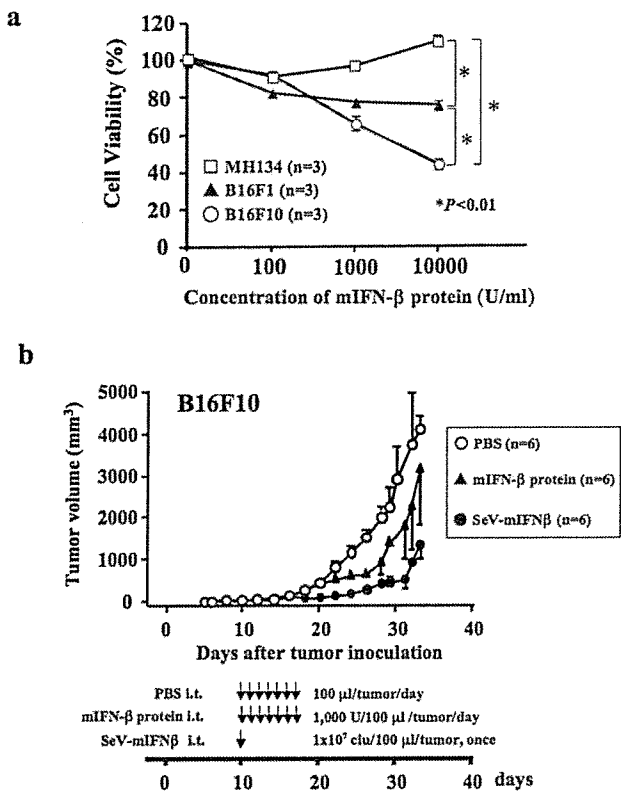

FIGURE 3. Antitumor activity of murine IFN-β against murine tumor cells in vitro (*a*) and in vivo (*b*). *a*, In vitro cytotoxicity of mIFN-β to murine melanomas (lower malignancy, B16F1; higher malignancy, B16F10) and a hepatocellular carcinoma (MH134). After 48-h culturing in the presence of mIFN-β protein, cell viability was assessed. The viability of MH134 (□) was not affected by mIFN-β, and in contrast, melanomas were sensitive to mIFN-β, suggested by the observed dose-dependent effects. Note that B16F10 (○) was more sensitive than B16F1(▲) to mIFN-β. *b*, Antitumor activity of protein (▲) and gene (●) therapies of mIFN-β in vivo. Ten days after tumor cell inoculation, when the established tumor was well-vascularized, protein or gene therapy was started according to the indicated regimen (*b*, bottom scheme: late treatment regimen).

Modulation of antitumor effects and immune responses to IFN-β-sensitive, established tumors by SeV/DCs expressing mIFN-β

Antitumor effect. IFN-β is known to be an antitumor cytokine via multiple mechanisms, including a direct antiproliferative effect, enhancement of NK cell activity, and up-regulation of tumor Ag and MHC class I and II (28). Therefore, we next asked whether DC therapy modulated by exogenous *mIFN-β* genes might affect the antitumor effect as well as immune responses against B16F10 melanoma.

First, we assessed MHC class I expression and its modulation by mIFN-β by flow cytometry analyses, because it is well-known that the expression of this molecule on tumor cells is required to be recognized by antitumor CTLs induced by cancer immunotherapy (29). As shown in Fig. 4*a*, the baseline expression of MHC class I ($H\text{-}2^k$) was high, and the level was not significantly changed by the treatment with mIFN-β. In contrast, both B16F1 and B16F10 cells expressed a very low level of MHC class I ($H\text{-}2^b$) at baseline, and after 48 h of culturing in the presence of 1000 U/ml mIFN-β protein, the level of MHC class I was dramatically increased. Together with Fig. 3*a*, these results might suggest that SeV/DCs expressing mIFN-β possibly enhanced the antitumor effect seen in the use of sole SeV/DCs.

To test this possibility, we next evaluated the antitumor effect SeV-mIFN-β/DCs, directly compared with those of LPS/DCs and SeV-GFP/DCs using established MH134 and B16F10 melanoma in vivo via later treatment regimen.

MH134 tumor

Tumor size (Fig. 4b). As expected, the tumor growth of established MH134 tumors was markedly inhibited irrespective of the types of DCs, namely, LPS/DCs, SeV-GFP/DCs, and SeV-mIFN-β/DCs, by the later treatment regimen (Fig. 4*b*).

Survival. No animal bearing MH134 was dead during experimental course.

Number of mice with tumor eliminated. No animal showed elimination of tumor irrespective of treatments.

B16F10 tumor

Tumor size (Fig. 4c). Evaluation of tumor size was relatively difficult, because 40% and all of untreated animals were dead within days 20 and 36, respectively (Fig. 4*c*, *upper panel*). In addition, death of animals was not corresponded to the size of tumor.

Survival. Although DC/lysate and LPS/DCs were likely to inhibit the growth of B16F10 tumors in vivo (Fig. 4*c*), both treatments did not contribute to the significant prolongation of the survival (Fig. 4*d*). In contrast, significant prolongation of survival over day 50 and tumor dormancy of animals bearing B16F10 melanoma were observed only in SeV/DC groups. A beneficial effect of the *IFN-β* transgene was seen in tumor size which was evaluated on day 50 (Fig. 4*e*).

Number of mice with tumor eliminated. No animal showed elimination of tumor irrespective of treatments.

Together, these results indicate that modification of the function of DCs by SeV expressing mIFN-β dramatically enhances the antitumor effect to tumor cells that are sensitive to IFN-β. Furthermore, these results strongly suggested that the modification of DC functions by SeV was beneficial on the survival, and exogenous IFN-β mainly contributes to the reduction of tumor volume.

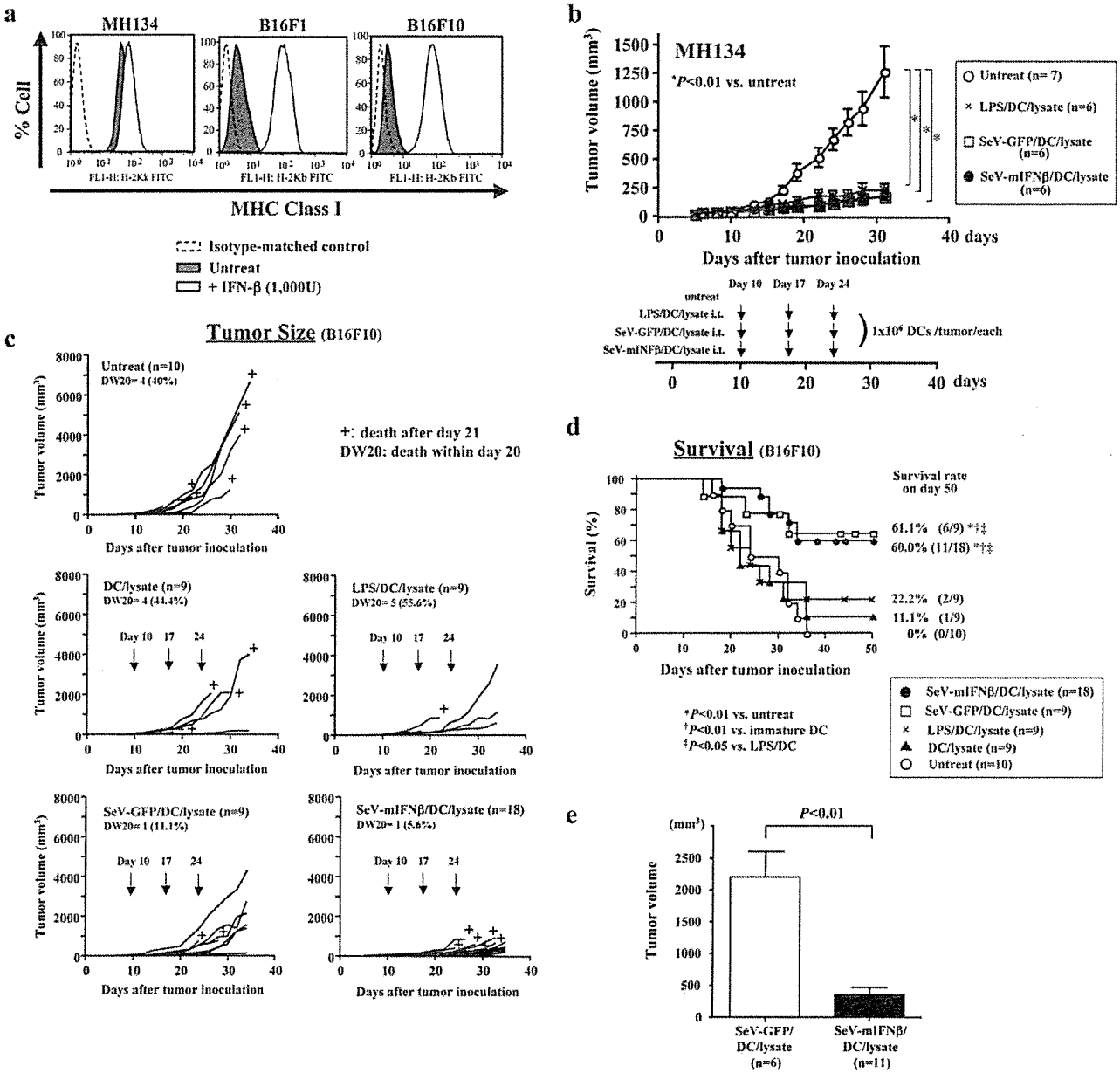

FIGURE 4. Tumor cell-dependent, divergent effects of SeV/DC immunotherapy expressing mIFN-β (late treatment regimen). *, $p < 0.01$. *a*, Flow cytometry analysis for MHC class I expression level of tumors treated with or without mIFN-β. After 48-h cultivation of tumor cells (MH134; H-2^k H-2^k, and B16F1, B16F10 melanoma; H-2^b) with or without mIFN-β, cells were subjected to the analysis. Note that the expression of MHC class I in both melanoma cells was very low, findings that were strongly up-regulated by mIFN-β treatment. *b*, Antitumor effect of SeV/DCs on a MH134 tumor, which was resistant to mIFN-β, with or without expression of mIFN-β in vivo. C3H/HeN mice were inoculated intradermally with 1×10^6 MH134 cells, which were resistant to mIFN-β, on day 0, and DC treatment was started at day 10 using 10^6 cells of LPS/DC (×), SeV-IFN-β/DC (●) or SeV-GFP/DC (□), as indicated in the bottom scheme. The data contains the results of all animals in two independent experiments. *c*, Time course of the volume of individual B16F10 tumors, a IFN-β-sensitive malignancy, treated with DC/lysate, LPS/DC/lysate, SeV-GFP/DC/lysate, or SeV-mIFN-β/DC/lysate. Untreated animals were used as a control group. DW20 indicates the number of death animals within day 20. +, Individual animals with death after day 21. *d*, Survival curve of the mice bearing B16F1 melanoma treated with various DCs. Significant prolongation of survival of mice bearing B16F10 melanoma was seen in SeV/DC groups, but not others. Data demonstrated were the total of four independent experiments. *e*, A graph indicating the effect of exogenous mIFN-β on tumor size of B16F10 melanoma. SeV/DC-treated animals surviving over 36 days were evaluated.

Immunological assessments

To explore the immunological effectors for the antitumor effects in DC therapy as well as gene therapy, we next focused on NK cells and CTL activities in mice bearing B16F10 and MH134 tumors treated by each method.

NK cells obtained from mice bearing B16F10 tumors treated with DCs, including LPS/DCs, SeV-GFP/DCs, and SeV-mIFN-β/DCs, did not show significant cell lysis activity. In contrast, NK cells from mice treated with direct i.t. vector injection of SeV-mIFN-β, aforementioned in Fig. 3*b*, showed apparently

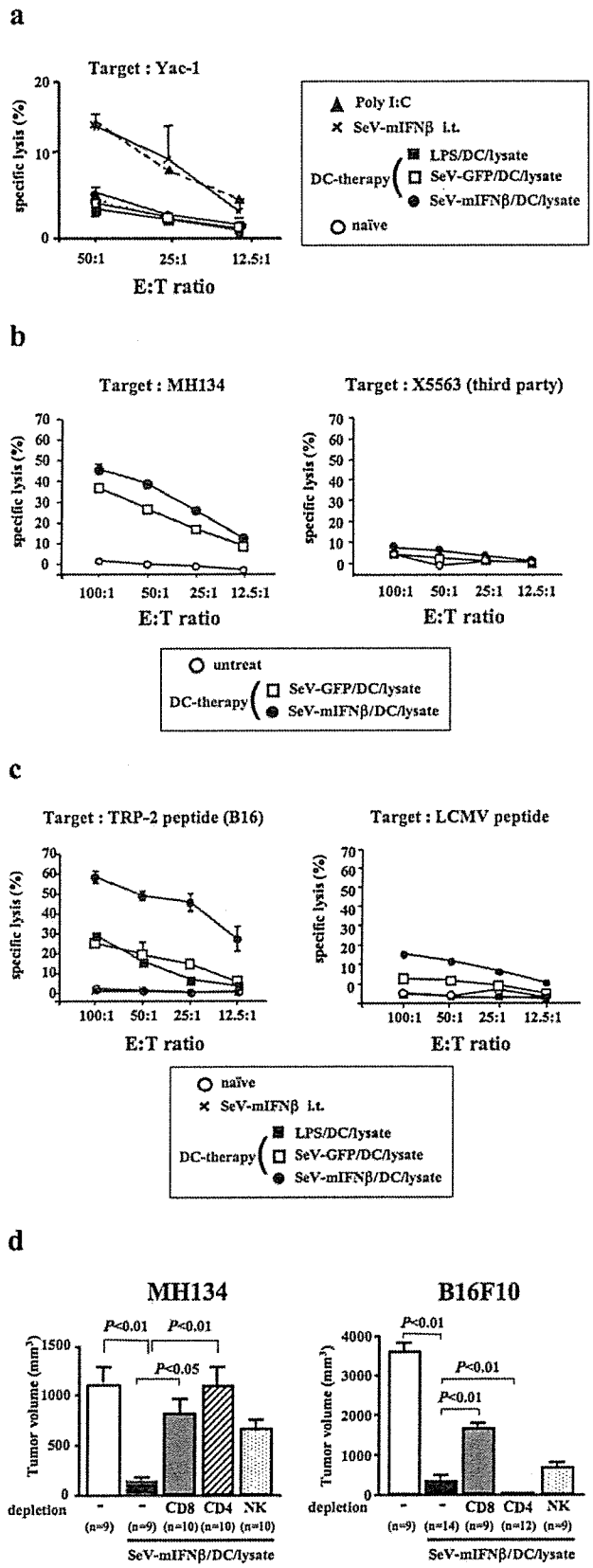

FIGURE 5. Effectors contributing to the antitumor effect of SeV/DC immunotherapy. *a*, Assessment of NK cell activity in B16F10 melanoma. Thirty-one days after B16F10 cell inoculation, splenocytes were isolated from the mice treated with SeV-GFP/DC/lysate (□), SeV-mIFN-β/DC/lysate (●), LPS/DC/lysate (■), or intratumoral direct injection of SeV-mIFN-β vector (X). The cytolytic function against ^{51}Cr-labeled YAC-1 targets was assessed by ^{51}Cr release. Splenocytes from the mouse, which were treated with 150 μl of poly I:C 24 h before the assay, were used as a positive control. *b*, Assessment for CTL activity of MH134. Induction of tumor-specific CTLs after i.t. administration of SeV-GFP/DC/lysate (□), SeV-mIFNβ/DC/lysate (●), and LPS/DC/lysate (■), which was repeated three times every week according to the late treatment regimen. Controls included tumor-bearing mice without any treatment (○). X5563 was also used as a target of a third party. Seven days after the last treatment, splenocytes were isolated and restimulated in vitro for 5 days with mitomycin C-treated MH134 cells, and cytolytic activity against ^{51}Cr-labeled targets was measured. The figure shows results from one of three similar experiments. *c*, Assessment for CTL activity of B16F10 cells. Induction of tumor-specific CTLs after i.t. administration of SeV-GFP/DC/lysate (□), SeV-mIFN-β/DC/lysate (●), and LPS/DC/lysate (■), which was repeated three times every week according to the late treatment regimen. Controls included tumor-bearing mice without any treatment (○). LCMV peptide was also used as a target of a third party. The method was same as above. *d*, Determination of immune cell subsets against MH134 or B16F10 responsible for the protective immunity induced by SeV-mIFN-β/DCs was Ab-mediated via an in vivo depletion analysis, as described in *Materials and Methods*. These bar graphs show the tumor volume on day 30 after inoculation of tumor cells. Anti-CD4 (GK1.5), anti-CD8 (53-6.72), or anti-asialo GM1 was i.p. injected according to the indicated schedule. In all animals, >98% of specific depletion of target cells in the spleen and lymph nodes was confirmed by flow cytometry (data not shown). The data contains all animals of two or three separate experiments.

strong cell lysis activity which was comparable to a positive control level (poly I:C) (Fig. 5*a*). These findings indicate that NK cells do not significantly contribute to the antitumor effect of DC therapy.

In contrast, CTLs from the splenocytes of mice showed opposite results, and demonstrated the comparable findings suggested in Fig. 4. In the case of CTLs against MH134 tumor cells, the expression of mIFN-β did not significantly affect the CTL activities induced by SeV/DC therapies (Fig. 5*b*, *left graph*). As a control experiment, X5563 tumor cells were used as a target, and showed negative result (Fig. 5*b*, *right panel*). In the case of TRP-2 peptide, a tumor-specific Ag of B16 melanoma as a target of CTLs obtained from spleens from mice bearing B16F10 melanoma, SeV/DCs showed a similar level of CTL activity compared with that seen in LPS/DCs, a finding that was markedly enhanced by SeV/DCs expressing mIFN-β (Fig. 5*c*, *left panel*). In this case, no significant CTL activity was detected in mice treated with direct vector injection of SeV-mIFN-β. In contrast, a relatively low level of background release was observed when third-party target (LCMV) was used (Fig. 5*d*, *right panel*).

These results thus indicate the significant contribution of IFN-β to the CTL activity for an IFN-β-sensitive B16F10 tumor but not for an insensitive MH134 tumor during DC therapy. Furthermore, these data suggest the distinct mechanisms of the antitumor effect of DC therapy compared with that of gene therapy, even when the same therapeutic gene, IFN-β, was used.

Effector cell subsets in DC therapies

To make it clear which subset(s) of cells is important for the antitumor effect of SeV-mIFN-β/DC therapy, we next conducted the effector cell depletion experiment by administration of each depletion Ab against CD8, CD4, and NK (by asialo-GM1) in mice with MH134 or B16F10 tumors treated with or without SeV-mIFN-β/DCs. The dose of each Ab was determined by our repeated preliminary experiments of FACS analyses that showed >98% of the target subject in some lymph nodes and the spleen (data not shown). The same lot of each Ab

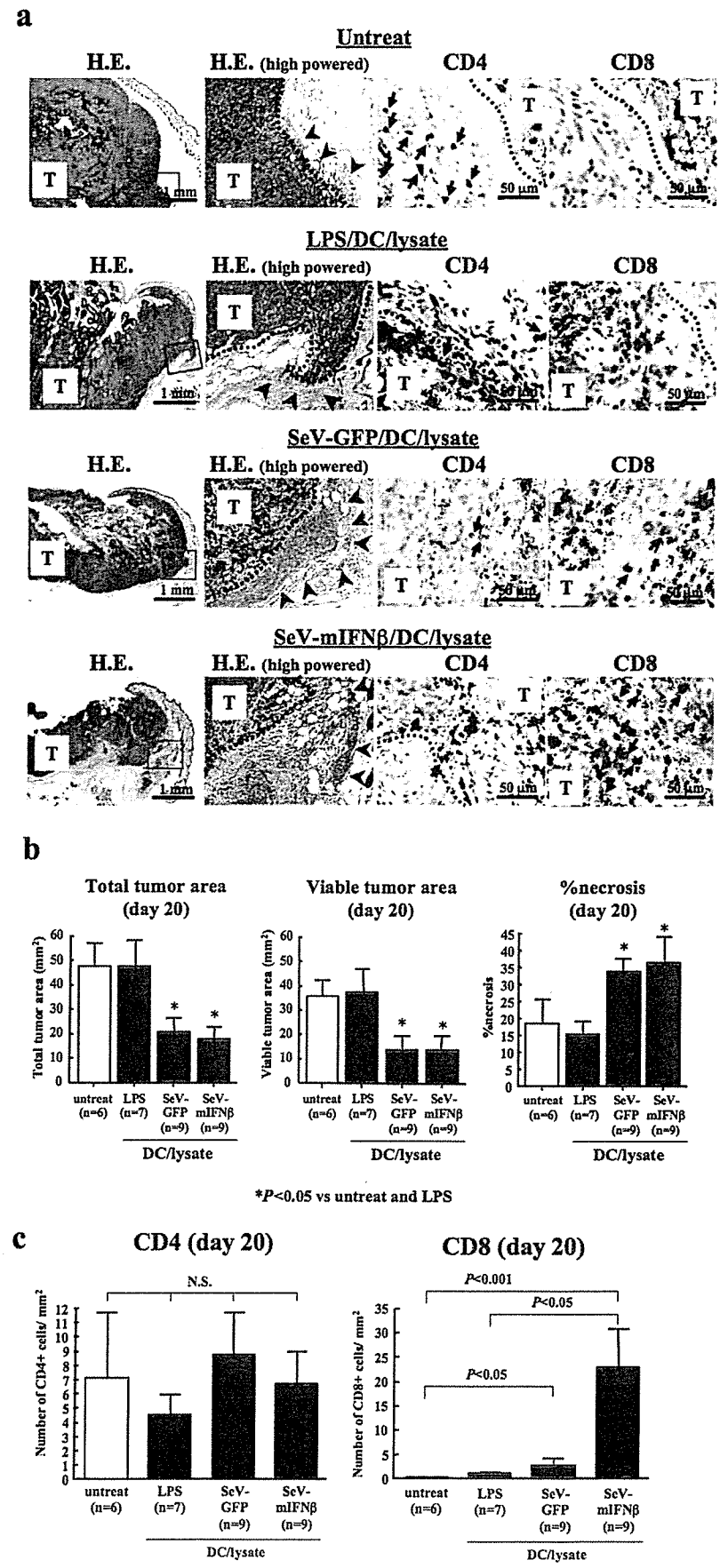

FIGURE 6. Histopathological and immunohistochemical examination of B16F10 tumors on day 20. Dot lines indicate the margin of tumors. *a*, Typical representative findings of the tumor environment on 20 days after inoculation of B16F10 treated with or without LPS/DC/lysate, SeV-GFP/DC/lysate, and SeV-mIFN-β/DC/lysate on days 10 and 17. Panels of H&E staining indicated as "high powered" are high powered view of their corresponding *left panels*. Arrowheads indicate the infiltration of chronic inflammatory cells, including lymphocytes and macrophages. Immunohistochemical positive reaction (red cytoplasm) of $CD4^+$ and $CD8^+$ cells are also demonstrated (arrows). These are representative of two separate studies using three to five mice per group. *b*, Bar graphs indicating the squares of total tumor area (*left*), viable tumor area (*middle*), and the ratio of necrotic area (*right*). H&E-stained sections were subjected to the computer-assisted square measurement. *c*, Bar graphs indicating the number of immunohistochemically $CD4^+$ and $CD8^+$ cells per mm^2 in the viable tumor area and peripheral tumor tissue.

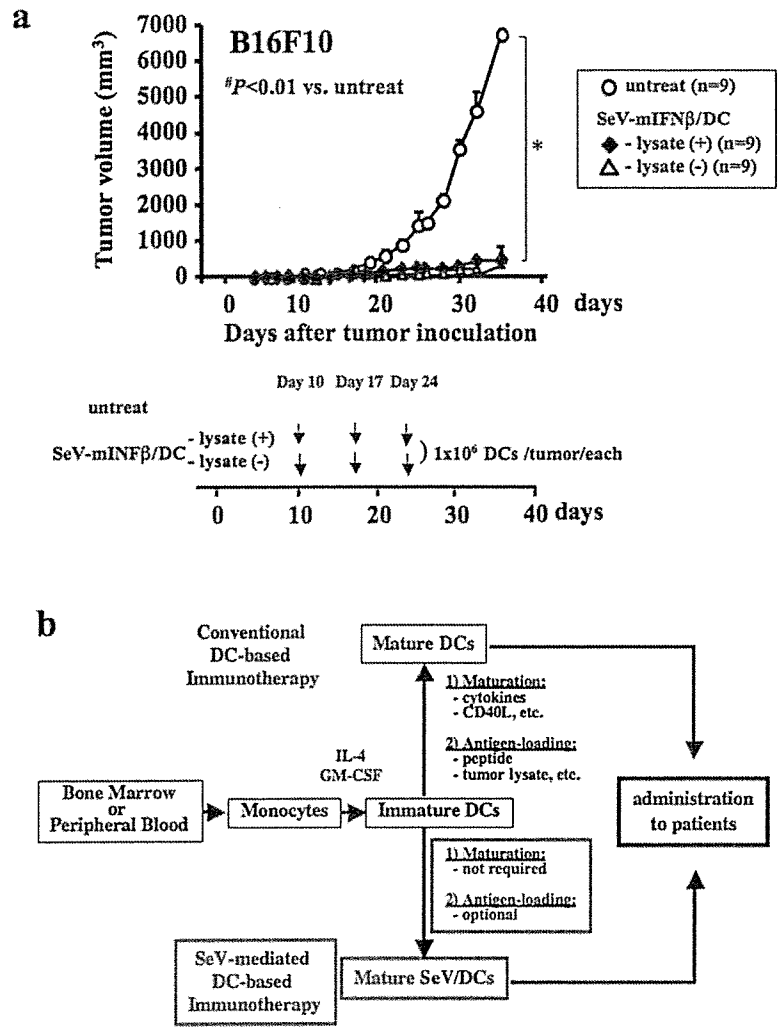

FIGURE 7. *a*, Requirement of ex vivo pulsation of tumor lysate during SeV-modified DC immunotherapy. The late treatment regimen against B16F10 melanoma was done via intratumor injection of SeV-mIFN-β/DC with or without tumor lysate. Ten days after B16F10 cell inoculation, i.t. injection of SeV-mIFN-β/DC pulsed with (♦) or without tumor lysate (△) was performed according to the protocol as indicated below. *, $p < 0.01$. *b*, Schematic representation of the comparison of conventional DC-based immunotherapy and that using SeV-modified DCs. The greatest advantages of the SeV/DC method are that: 1) there is no requirement of a specific stimulus to induce strong DC activation representatively, and 2) Ag-loading is not critical when SeV/DC is administered directly to tumors.

was used throughout the experiments. The tumor size was evaluated every day, and the data on day 30 are presented.

As shown in Fig. 5*c*, in the case of MH134 tumors, as expected, depletion either of $CD4^+$ T cells or $CD8^+$ T cells almost totally abrogated the antitumor effect induced by SeV-mIFN-β/DCs, and the depletion of NK cells partly canceled the effect (Fig. 5*c*, *left graph*). These findings indicate that the tumor-specific CTL as well as the helper function of CD4 are absolutely necessary to the therapeutic effect of SeV-mIFN-β/DCs, and further, NK cell activity is also involved in the effect.

In the case of B16F10 melanoma, in contrast, such depletion studies demonstrated unexpected results. Depletion of $CD8^+$ T cells during therapy partially cancelled the protective immunity induced by SeV-mIFN-β/DCs; however, mice depleted of NK cells during therapy showed no significant effect (Fig. 5*c*, *right graph*), data supported by the cell lysis analysis shown in Fig. 5*a*. When $CD4^+$ T cells were depleted, however, the antitumor effect of SeV-mIFN-β/DCs was markedly and significantly enhanced, indicating that the net effect of $CD4^+$ T cells was to function as a helper for tumors rather than providing antitumor immunity. These data might possibly reflect the function of regulatory T cells ($CD4^+$ $CD25^+$ T cells) in the $CD4^+$ T cell subset (30).

These findings confirm that $CD8^+$ T cells were the ubiquitous and predominant effector cells in antitumor immunity for both MH134 and B16 melanoma, even though their quantitative contribution may vary depending on the tumor type.

Histological and immunohistochemical assessments for modification of tumor environment

Next, we histopathologically examined the B16F10 melanoma tumor environment, including tumor area (viable tumor and ratio of necrosis) and infiltration of CD4 and CD8 T lymphocytes, using another set of DC therapy experiments. At that time, DC therapy was done on days 10 and 17, and the tumor was harvested on day 20. Four of 10 animals of the untreated group and 3 of 10 of the LPS/DC group but not all SeV/DC groups were dead within day 20.

Histological examination suggested that the infiltration of inflammatory cells around tumor was more pronounced in DC therapy groups (Fig. 6*a*), and interestingly, more reduction of tumor area and viable tumor area was seen in the SeV/DC groups, but not in the LPS group (Fig. 6*b*, *left* and *middle graphs*). In contrast, the ratio of tumor necrosis was more pronounced in the SeV/DC groups (Fig. 6*b*, *right graph*), and these findings were observed irrespective of use of SeV/DCs expressing IFN-β.

Immunohistochemistry demonstrated more frequent infiltration of CD8 T lymphocytes into tumor and surrounding s.c. tissue by treatment of SeV-mIFN-β/DCs compared with other

groups (Fig. 6*c*, *right graph*), a comparable finding obtained in Fig. 5*c*, while no significant difference was determined in CD4 T lymphocyte infiltration among all groups tested (Fig. 6*c*, *left panel*).

These results thus suggest the split mechanisms of SeV-mediated modulation of DC function and expression of IFN-β on the antitumor effect of B16F10 melanoma.

No requirement of Ag loading during ex vivo culture of SeV-mIFN-β/DCs

Finally, we investigated the requirement of ex vivo Ag loading during the culturing of SeV-mIFN-β/DCs, because ex vivo Ag loading has been considered to be an essential step in inducing tumor-specific immunity (31, 32). To assess this, we used a late treatment regimen against B16F10 melanoma via i.t. injection of SeV-mIFN-β/DC with or without tumor lysate.

As shown in Fig. 7, the therapeutic effect of SeV-mIFN-β/DCs was not affected by ex vivo Ag-loading when DCs were injected i.t., indicating that the antitumor effect can be led by direct i.t. injection of SeV-mIFN-β/DCs without any supplementation of ex vivo Ags.

Discussion

During the last decade, clinical trials of DC-based immunotherapy have revealed a relatively limited clinical outcome against intractable malignancies (3). These early results do not always suggest the limited potential of DC-based immunotherapy, however, because there are still a number of issues to be clarified, including how to monitor the activation of DCs, which route and with what frequency DCs should be administered, how Ags should be targeted, and which malignancy and what stages of malignancy should be selected (2). Physicians and scientists should clarify these points and apply the answers to the basic mechanisms of tumor biology and DC therapy, because no one knows, at present, the optimized potentials of DC-based cancer immunotherapy in clinical settings.

We here assessed the antitumor potential of a novel DC-activating modality, rSeV, and directly compared it to that of LPS, which is not relevant clinically but experimentally shows the high performance in terms of DC activation. Key observations obtained in this study were as follows: 1) SeV not only transduced foreign genes to immature DCs but also led them a highly activated state that was comparable to that induced by LPS, 2) the bioactive potential of SeV/DCs as an antitumor agent was seen in tumor-bearing mice in vivo, 3) complete elimination of an established low malignancy tumor, IFN-β-sensitive B16F1, could be found via an early treatment regimen using SeV-GFP/DCs, findings enhanced by SeV/DCs expressing mIFN-β, 4) SeV/DC therapy was likely to be more effective than protein and gene therapies, 5) distinct mechanisms of antitumor effects were suggested between gene therapy and SeV/DC therapy, even though both used the same therapeutic gene, mIFN-β, and 6) the process of ex vivo Ag loading was not important in the therapeutic effect of SeV-mIFN-β/DCs when they were injected i.t.

Because this is the first demonstration of a negative strand RNA virus-mediated DC activation for cancer immunotherapy, there are still a number of unanswered questions regarding this system. However, it should be true that SeV is a strong and important modality for activating DCs which may be useful for cancer immunotherapy.

At present, the precise molecular and cellular mechanisms of activation of DCs by SeV are not well-understood. In this study, we demonstrated that DCs treated by SeV secrete several inflammatory cytokines, including IL-1β, IL-6, and TNF-α, that are strong activators to DCs in mixture (33); however, no knowledge of how DCs exposed to SeV express these cytokines is available at present. A recent important report indicated that DCs treated with SeV produce multiple proinflammatory cytokines independent of TLRs and their adaptors, including MyD88 (34), unlike LPS, CpG (35), or OK-432 (36), which stimulate DCs through a TLR-dependent mechanism.

An important finding obtained in the current study is that stronger antitumor effect on B16 melanomas was seen in SeV-modified DCs compared with that seen in LPS/DCs, even though the expression of costimulatory molecules and typical Th1 cytokines of SeV/DCs did not always reach the levels of LPS/DCs. These results strongly suggest the complex mechanism of antitumor effect; namely, antitumor activity of DC immunotherapy cannot generally be predicted by the expression of these molecules. We are now assessing this point extensively.

An essential finding in the current study is that SeV-mIFN-β/DC therapy was considerably effective for treating IFN-β-sensitive tumors, B16 melanomas, even in the case of the highly malignant B16F10 subtype. More importantly, this effect was shown by the later treatment regimen, on day 10, when the tumor was 7–9 mm in diameter and well-vascularized as revealed by histopathological assessment (data not shown). Because "there are no cancer vaccine models that reproducibly demonstrate that vascularized tumors can be rejected" at present, as noted by Rosenburg et al. (3), SeV-mIFN-β/DC therapy may be an important candidate for overcoming the current limitation in immunotherapy for melanoma in the clinical setting.

An important question raised in this study is what is the precise mechanism(s) of SeV-mIFN-β/DC therapy against B16F10 melanoma? Fig. 5 suggested that NK cells seemed not to be important in this case, while they did actually show the antitumor effect seen in MH134, at least in part. A $CD8^+$ cell depletion study demonstrated $CD8^+$ CTLs as major effectors for SeV-mIFN-β/DC therapy for B16F10 melanoma, and mIFN-β expression in DCs enhanced the CTL activity (Fig. 5*b*). These findings show that the direct cytotoxicity of mIFN-β and the induction of $CD8^+$ CTLs may be major players in the antitumor effect of SeV-mIFN-β/DC therapy against B16F10 melanoma, which may be modified by the expression of MHC class I in tumor cells. This explains why the antitumor effect against MH134, which was insensitive to mIFN-β, was not modified by the use of SeV-mIFN-β/DCs. Modulation of MHC class I expression is an important part of antitumor immunity; loss or down-regulation of MHC class I is an important mechanism for the tumor's escape from the host immune system, resulting in the peripheral tolerance (37–39).

In addition, it is of interest that our current study demonstrated that distinct beneficial effect of SeV/DCs and those expressing exogenous IFN-β; namely, modification of DC function by SeV contributed to the survival and increase of the tumor necrotic area, and exogenous expression of mIFN-β significantly enhanced CTL activity and increased recruitment of $CD8^+$ T cells. These results thus suggest the modulation of host immune response to malignancies via DC immunotherapy by mIFN-β; however, exact mechanisms of apparent improvement of survival and increase of necrotic area via SeV/DCs without exogenous gene, that was not seen by LPS/DCs, are still unknown. One possible explanation is the effect caused by DC-derived endogenous type I IFNs, which were not detected by LPS treatment, caused by viral transduction. According to our careful observation, death of mice bearing B16F10 within day 20 was caused by extensive hemorrhage from ulceration of tumors. It has been shown that low-dose type I IFNs,

including IFN-β, reduced tumor vasculature, a possible mechanism of reduced rate of hemorrhage. This is likely because some previous studies demonstrated that the antiangiogenic activity of mIFN-β did not show apparent dose response (40), a comparable finding obtained in the current study. Such multiple functions of IFN-β would be favorable for cancer immunotherapy, further studies should be done to assess the precise mechanism of action of IFN-β in clinical settings.

One more question raised in this study involves the role of $CD4^+$ T cells in antitumor immunity, which showed conflicting results between two different tumors, namely, depletion of $CD4^+$ cells completely canceled the antitumor effect of SeV-mIFN-β/DCs against MH134 tumors and, inversely, markedly enhanced that against B16F10 melanoma. It is still premature, at present, to draw a conclusion, but we believe a possible contribution of $CD4^+/CD25^{high}$ regulatory T lymphocytes (T-reg) may be involved. Recent progress in knowledge about how tumors escape from host immune surveillance shows an essential contribution of T-reg in tumor immunity (41). The distinct effects of CD4 depletion between two different tumor types, however, may imply that the findings depend on the cell sources, so further study is called for to determine the tumor and/or DC factors contributing to the function of T-reg.

Can SeV/DC show a significant anticancer effect over that seen using current DC immunotherapy in clinical use? It may be premature to suggest this, however, the present study implies some important advantages of SeV/DC-based cancer immunotherapy. In this study, we showed that SeV/DC therapy revealed a strong antitumor effect over that seen with the use of LPS/DCs, which can produce one of the strongest anticancer effects in experimental conditions, and these findings suggest that the therapeutic potential of SeV/DCs warrants further studies, including clinical trials. Because mass production of good manufacturing practice grade SeV is now available, it is not a long way to move SeV/DC-mediated cancer immunotherapy to clinical practice.

In summary, we demonstrated that SeV-modified DCs showed antitumor effects on established tumors in vivo; and we would therefore like to propose a concept for tumor immunotherapy using SeV-modified DCs known as "immunostimulatory virotherapy." The current study results strongly suggest that SeV/DC-based cancer immunotherapy may be an important alternative therapy and that the technique warrants further investigation in research as well as in clinical trials.

Acknowledgments

We thank Hiroshi Fujii for tissue processing and immunohistochemistry, and Chie Arimatsu for her help on animal experiments.

Disclosures

The authors have no financial conflict of interest.

References

1. Zitvogel, L., J. I. Mayordomo, T. Tjandrawan, A. B. DeLeo, M. R. Clarke, M. T. Lotze, and W. J. Storkus. 1996. Therapy of murine tumors with tumor peptide-pulsed dendritic cells: dependence on T cells, B7 costimulation, and T helper cell 1-associated cytokines. *J. Exp. Med.* 183: 87–97.
2. Berzofsky, J. A., M. Terabe, S. Oh, I. M. Belyakov, J. D. Ahlers, J. E. Janik, and J. C. Morris. 2004. Progress on new vaccine strategies for the immunotherapy and prevention of cancer. *J. Clin. Invest.* 113: 1515–1525.
3. Rosenberg, S. A., J. C. Yang, and N. P. Restifo. 2004. Cancer immunotherapy: moving beyond current vaccines. *Nat. Med.* 10: 909–915.
4. Banchereau, J., and R. M. Steinman. 1998. Dendritic cells and the control of immunity. *Nature* 392: 245–252.
5. Hsu, F. J., C. Benike, F. Fagnoni, T. M. Liles, D. Czerwinski, B. Taidi, E. G. Engleman, and R. Levy. 1996. Vaccination of patients with B-cell lymphoma using autologous antigen-pulsed dendritic cells. *Nat. Med.* 2: 52–58.
6. Nestle, F. O., S. Alijagic, M. Gilliet, Y. Sun, S. Grabbe, R. Dummer, G. Burg, and D. Schadendorf. 1998. Vaccination of melanoma patients with peptide- or tumor lysate-pulsed dendritic cells. *Nat. Med.* 4: 328–332.
7. Timmerman, J. M., and R. Levy. 1998. Melanoma vaccines: prim and proper presentation. *Nat. Med.* 4: 269–270.
8. Kim, D. 2000. Replication-selective oncolytic adenoviruses: virotherapy aimed at genetic targets in cancer. *Oncogene* 19: 6660–6669.
9. Noguchi, Y., K. Sawaizumi, K. Ishiwara, and T. Saito. 1960. Virotherapy of skin cancers. I. Clinical effect of purified vaccine lymph on skin cancers. *Yokohama Med. Bull.* 11: 241–249.
10. Yonemitsu, Y., C. Kitson, S. Ferrari, R. Farley, U. Griesenbach, D. Judd, R. Steel, P. Scheid, J. Zhu, P. K. Jeffery, et al. 2000. Efficient gene transfer to airway epithelium using recombinant Sendai virus. *Nat. Biotechnol.* 18: 970–973.
11. Masaki, I., Y. Yonemitsu, K. Komori, H. Ueno, Y. Nakashima, K. Nakagawa, M. Fukumura, A. Kato, M. K. Hasan, Y. Nagai, et al. 2001. Recombinant Sendai virus-mediated gene transfer to vasculature: a new class of efficient gene transfer vector to the vascular system. *FASEB J.* 15: 1294–1296.
12. Tsutsumi, N., Y. Yonemitsu, Y. Shikada, M. Onimaru, M. Tanii, S. Okano, K. Kaneko, M. Hasegawa, M. Hashizume, Y. Maehara, and K. Sueishi. 2004. Essential role of PDGFRα-p70S6K signaling in mesenchymal cells during therapeutic and tumor angiogenesis in vivo: role of PDGFRα during angiogenesis. *Circ. Res.* 94: 1186–1194.
13. Nagai, Y. 1999. Paramyxovirus replication and pathogenesis: reverse genetics transforms understanding. *Rev. Med. Virol.* 9: 83–99.
14. Markwell, M. A., L. Svennerholm, and J. C. Paulson. 1981. Specific gangliosides function as host cell receptors for Sendai virus. *Proc. Natl. Acad. Sci. USA* 78: 5406–5410.
15. Moyer, S. A., S. C. Baker, and J. L. Lessard. 1986. Tubulin: a factor necessary for the synthesis of both Sendai virus and vesicular stomatitis virus RNAs. *Proc. Natl. Acad. Sci. USA* 83: 5405–5409.
16. Jin, C. H., K. Kusuhara, Y. Yonemitsu, A. Nomura, S. Okano, H. Takeshita, M., Hasegawa., K. Sueishi, and T. Hara T. 2003. Recombinant Sendai virus provides a highly efficient gene transfer into human cord blood-derived hematopoietic stem cells. *Gene Ther.* 10: 272–277.
17. Harada, N., M. Shimada, S. Okano, T. Suehiro, Y. Soejima, Y. Tomita, and Y. Maehara. 2004. IL-12 gene therapy is an effective therapeutic strategy for hepatocellular carcinoma in immunosuppressed mice. *J. Immunol.* 173: 6635–6644.
18. Inaba, K., M. Inaba, N. Romani, H. Aya, M. Deguchi, S. Ikehara, S. Muramatsu, and R. M. Steinman. 1992. Generation of large numbers of dendritic cells from mouse bone marrow cultures supplemented with granulocyte/macrophage colony-stimulating factor. *J. Exp. Med.* 176: 1693–1702.
19. Jackson, S. H., C. Alicea, J. W. Owens, C. L. Eigsti, and H. L. Malech. 2002. Characterization of an early dendritic cell precursor derived from murine lineage-negative hematopoietic progenitor cells. *Exp. Hematol.* 30: 430–439.
20. Spang-Thomsen, M., A. Nielsen, and J. Visfeldt. 1980. Growth curves of three human malignant tumors transplanted to nude mice. *Exp. Cell Biol.* 48: 138–154.
21. Bloom, M. B., D. Perry-Lalley, P. F. Robbins, Y. Li, M. el-Gamil, S. A. Rosenberg, and J. C. Yang. 1997. Identification of tyrosinase-related protein 2 as a tumor rejection antigen for the B16 melanoma. *J. Exp. Med.* 185: 453–459.
22. Bellone, M., D. Cantarella, P. Castiglioni, M. C. Crosti, A. Ronchetti, M. Moro, M. P. Garancini, G. Casorati, and P. Dellabona. 2000. Relevance of the tumor antigen in the validation of three vaccination strategies for melanoma. *J. Immunol.* 165: 2651–2656.
23. Dialynas, D. P., Z. S. Quan, K. A. Wall, A. Pierres, J. Quintans, M. R. Loken, M. Pierres, and F. W. Fitch. 1983. Characterization of the murine T cell surface molecule, designated L3T4, identified by monoclonal antibody GK1.5: similarity of L3T4 to the human Leu-3/T4 molecule. *J. Immunol.* 131: 2445–2451.
24. Ledbetter, J. A., and L. A. Herzenberg. 1979. Xenogeneic monoclonal antibodies to mouse lymphoid differentiation antigens. *Immunol. Rev.* 47: 63–90.
25. Sauter, B., M. L. Albert, L. Francisco, M. Larsson, S. Somersan, and N. Bhardwaj. 2000. Consequences of cell death: exposure to necrotic tumor cells, but not primary tissue cells or apoptotic cells, induces the maturation of immunostimulatory dendritic cells. *J. Exp. Med.* 191: 423–433.
26. Song, W., and R. Levy. 2005. Therapeutic vaccination against murine lymphoma by intratumoral injection of naive dendritic cells. *Cancer Res.* 65: 5958–5964.
27. Nagatani, T., S. Ichiyama, K. Miyakawa, and M. Uchiyama. 1992. Malignant melanoma treated with natural interferon α and β and DAV. *Eur. J. Cancer* 28A: 1774.
28. Hansen, R. M., and E. C. Borden. 1992. Current status of interferons in the treatment of cancer. *Oncology* 6: 19–24.
29. Vertuani, S., A. De Geer, V. Levitsky, P. Kogner, R. Kiessling, and J. Levitskaya. 2003. Retinoids act as multistep modulators of the major histocompatibility class I presentation pathway and sensitize neuroblastomas to cytotoxic lymphocytes. *Cancer Res.* 63: 8006–8013.
30. Steitz, J., J. Bruck, J. Lenz, J. Knop, and T. Tuting, T. 2001. Depletion of $CD25^+CD4^+$ T cells and treatment with tyrosinase-related protein 2-transduced dendritic cells enhance the interferon α-induced, $CD8^+$ T-cell-dependent immune defense of B16 melanoma. *Cancer Res.* 61: 8643–8646.
31. Nestle, F. O. 2000. Dendritic cell vaccination for cancer therapy. *Oncogene* 19: 6673–6679.
32. Strome, S. E., S. Voss, R. Wilcox, T. L. Wakefield, K. Tamada, D. Flies, A. Chapoval, J. Lu, J. L. Kasperbauer, D. Padley, et al. 2002. Strategies for

antigen loading of dendritic cells to enhance the antitumor immune response. *Cancer Res.* 62: 1884–1889.

33. Jonuleit, H., U. Kuhn, G. Muller, K. Steinbrink, L. Paragnik, E. Schmitt, J. Knop, and A. H. Enk. 1997. Pro-inflammatory cytokines and prostaglandins induce maturation of potent immunostimulatory dendritic cells under fetal calf serum-free conditions. *Eur. J. Immunol.* 27: 3135–3142.
34. Lopez, C. B., B. Moltedo, L. Alexopoulou, L. Bonifaz, R. A. Flavell, and T. M. Moran. 2004. TLR-independent induction of dendritic cell maturation and adaptive immunity by negative-strand RNA viruses. *J. Immunol.* 173: 6882–6889.
35. Hiraoka, K., S. Yamamoto, S. Otsuru, S. Nakai, K. Tamai, R. Morishita, T. Ogihara, and Y. Kaneda. 2004. Enhanced tumor-specific long-term immunity of hemagglutinating virus of Japan-mediated dendritic cell-tumor fused cell vaccination by coadministration with CpG oligodeoxynucleotides. *J. Immunol.* 173: 4297–4307.
36. Nakahara, S., T. Tsunoda, T. Baba, S. Asabe, and H. Tahara. 2003. Dendritic cells stimulated with a bacterial product, OK-432, efficiently induce cytotoxic T lymphocytes specific to tumor rejection peptide. *Cancer Res.* 63: 4112–4118.
37. Cromme, F. V., J. Airey, M. T. Heemels, H. L. Ploegh, P. J. Keating, P. L. Stern, C. J. Meijer, and J. M. Walboomers. 1994. Loss of transporter protein, encoded by the *TAP-1* gene, is highly correlated with loss of HLA expression in cervical carcinomas. *J. Exp. Med.* 179: 335–340.
38. Cohen, E. P., and T. S. Kim. 1994. Neoplastic cells that express low levels of MHC class I determinants escape host immunity. *Semin. Cancer Biol.* 5: 419–428.
39. Speiser, D. E., R. Miranda, A. Zakarian, M. F. Bachmann, K. McKall-Faienza, B. Odermatt, D. Hanahan, R. M. Zinkernagel, and P. S. Ohashi. 1997. Self antigens expressed by solid tumors do not efficiently stimulate naive or activated T cells: implications for immunotherapy. *J. Exp. Med.* 186: 645–653.
40. Streckm, C. J., Y. Zhang, R. Miyamoto, J. Zhou, C. Y. C. Ng, A. C. Nathwani, and A. M. Davidoff. 2004. Restriction of neuroblastoma angiogenesis and growth by interferon-α/β. *Surgery* 136: 183–189.
41. O'Garra, A., and P. Vieira. 2004. Regulatory T cells and mechanisms of immune system control. *Nat. Med.* 10: 801–805.

Sendai Virus-Mediated Gene Delivery into Hepatocytes *via* Isolated Hepatic Perfusion

Shigeo FUJITA,[a] Akiko EGUCHI,[b,c] Jun OKABE,[b,c] Atsushi HARADA,[d,e,i] Katsunori SASAKI,[f] Naoko OGIWARA,[f] Yoshifumi INOUE,[a] Toshinori ITO,[a] Hikaru MATSUDA,[a] Kazunori KATAOKA,[d,e] Atsushi KATO,[g] Mamoru HASEGAWA,[h] and Mahito NAKANISHI*,[b]

[a] *Department of Surgery, E1, Osaka University Graduate School of Medicine; Suita, Osaka 565–0871, Japan:* [b] *Gene Function Research Center, National Institute of Advanced Industrial Science and Technology (AIST); Tsukuba, Ibaraki 305–8562, Japan:* [c] *Japan Society for the Promotion of Science; Chiyoda-ku, Tokyo 102–8471, Japan:* [d] *Department of Material Science, School of Engineering, Tokyo University; Bunkyo-ku, Tokyo 113–8656, Japan:* [e] *CREST, Japan Science and Technology Agency; Kawaguchi, Saitama 332–0012, Japan:* [f] *Department of Histology and Embryology, Organ Technology, Shinshu University School of Medicine; Matsumoto, Nagano 390–8621, Japan:* [g] *Department of Virology 3, National Institute of Infectious Diseases; Musashi-Murayama, Tokyo 208–0011, Japan:* [h] *DNAVEC Corporation; Tsukuba, Ibaraki 305–0856, Japan: and* [i] *Department of Applied Material Science, School of Engineering, Osaka Prefecture University; Sakai, Osaka 599–8531, Japan.*

Received March 10, 2006; accepted May 1, 2006; published online May, 12, 2006

The recombinant Sendai virus vector is a promising tool for human gene therapy, capable of inducing high-level expression of therapeutic genes in tissue cells *in situ*. The target tissues include airway epithelium, blood vessels, skeletal muscle, retina and the central nervous system, but application to hepatic tissues has not yet been achieved, because direct intraportal injection of the vector is not feasible. We report an efficient and harmless procedure of gene delivery by recombinant Sendai virus into rat parenchymal hepatocytes, based on isolated hepatic perfusion with controlled inflow. Critical parameters for successful hepatic gene delivery are a brief preperfusion period (25 °C, 5 min); appropriate vector concentration in the perfusate (10^7 pfu/ml); moderate portal vein pressure (12 mmHg) and a brief hyperthermic postperfusion period (42 °C, 5 min). Under these optimized conditions, marker genes were expressed in most parenchymal hepatocytes without significant damage to hepatic tissues. Furthermore, expression of the marker genes was undetectable in nonhepatic tissues, including the gonads, indicating that this approach strictly targets hepatic tissues and thus offers good clinical potential for human gene therapy.

Key words gene delivery; hepatic perfusion; Sendai virus vector; vector targeting

The Sendai virus is a nonsegmented negative strand RNA virus belonging to the *Paramyxoviridae*.[1] It has a unilamellar lipoid envelope encapsulating the nucleocapsid (RNA–protein complex), and infects the host cell by delivering the nucleocapsid *via* fusion between the envelope and the cell membrane.[1] Recombinant Sendai virus has received attention as a unique viral vector for human gene therapy, capable of producing a large amount of therapeutic proteins,[2,3] with exceptionally broad cell and tissue specificities.[4] For example, recombinant Sendai virus has been used successfully to deliver therapeutic genes *in situ* into airway epithelium,[5] blood vessels,[6] skeletal muscle,[7] retina[8] and the central nervous system[9] of various animal species. This broad host specificity partly depends on the early stage of infection, using sialic acid, a ubiquitous component of the animal cell membrane, as a primary receptor.[10] Nevertheless, the application of this vector to the parenchymal hepatocyte, an important target cell in gene therapy for treating metabolic diseases, has not yet been established.

As the native Sendai virus can infect nondividing parenchymal hepatocytes *in vitro*,[4,9] derivative vectors are potentially applicable to the hepatic tissue *in vivo*. However, direct *intravenous* or *intraportal* injection of Sendai virus vectors is not feasible because of their hemagglutinating and hemolytic activities: the injected vectors immediately aggregate and destroy red blood cells, and may form a harmful blood coagulation. Furthermore, Sendai virus particles (230 nm in diameter) are larger than the mesh of the hepatic sinusoids (*ca.* 100 nm), a physiological sieve that restricts the access of large serum components to parenchymal hepatocytes;[11] this also hinders their application to the hepatic tissue.

In this article, we describe a procedure of isolated hepatic perfusion that enables reproducible and tissue-specific gene delivery by Sendai virus vectors. Isolated hepatic perfusion is a surgical procedure originally developed for treating nonresectable liver tumors by regional high-dose administration of anticancer drugs,[12,13] and has been used for delivering gene transfer vectors into hepatic tissues.[14—17] This procedure is useful for administrating Sendai virus vectors because a brief preperfusion can flush interfering blood cells from the hepatic tissue. Furthermore, perfusion under controlled portal pressure alters the mean mesh size of the hepatic sinusoids so that the Sendai virus particles can path through this physiological sieve. As isolated hepatic perfusion has been successfully applied to chemotherapy for nonresectable hepatic tumors in clinical trials, this approach should be feasible for human gene therapy.

MATERIALS AND METHODS

Purification and Physical Characterization of Sendai Virus Vectors Recombinant Sendai viruses carrying the firefly luciferase gene (SeV-luc)[18] and the gene for enhanced green fluorescent protein (SeV-EGFP)[19] were propagated by inoculating 100 μl of the diluted working virus seed contain-

To whom correspondence should be addressed. e-mail: mahito-nakanishi@aist.go.jp

ing *ca.* 10 plaque-forming units (pfu) of the virus into the chorio-allantoic cavity of 10-d-old fertilized domestic chicken eggs. After 72 h incubation, the viral particles were recovered from the chorio-allantoic fluid by high-speed centrifugation and suspended in BSS buffer (150 mM NaCl, 10 mM Tris–HCl, pH 7.6) as previously described.[20]

Viral particles were purified using sucrose two-step centrifugation (20% and 50% sucrose in BSS; 60000 ***g*** for 60 min at 4 °C in a Beckman SW28Ti rotor), and recovered from the interface between the sucrose layers.[21] The purified viral particles were then subjected to gel filtration for sizing,[22] using Sephacryl S1000 (2.0 45 cm diameter columns; Amersham Biotechnology, Piscataway, New Jersey, U.S.A.) as a medium, with HBS (150 mM NaCl, 10 mM HEPES–NaOH, pH 7.6) as running buffer. Gel filtration using Sephacryl S1000 has been successfully used for sizing large unilamellar liposomes with diameters of 200—400 nm.[22] The flow rate was kept at 0.1 ml/min, and aliquots of 2 ml were collected. All purification procedures were performed under a sterile environment.

The diameter of viral particles in each fraction was determined by the cumulant method using a dynamic light scattering spectrophotometer (model DLS-700, Otsuka Electronics Co., Ltd., Osaka, Japan).[23] The infectious titer of the purified virus was determined by plaque assays using $LLCMK_2$ cells.[24] Purified viral particles were frozen at 80 °C in the presence of 10% dimethyl sulfoxide.

For examining the purified Sendai virus particles under scanning electron microscopy, the samples were fixed in 2.5% glutaraldehyde in 0.1 M phosphate buffer (pH 7.0) (2 h at 25 °C, then 14 h at 4 °C), and trapped on Nuclepore polycarbonate membrane filters (pore size 0.05 μm, Whatman Inc., Clifton, NJ, U.S.A.). The samples were then dehydrated, dried, coated with an osmium plasma coater (thickness *ca.* 2 μm) and examined as described.[25]

Surgical Procedure for Isolated Hepatic Perfusion Specific pathogen free, 8- to 10-week-old male Wistar rats (Japan SLC, Shizuoka, Japan) were used throughout the study. All the animal experiments were performed according to our institutional guidelines for the care and use of laboratory animals. Anesthesia was induced and maintained using ether inhalation.

Abdominal exposure was carried out through a midline incision. The liver and the suprahepatic caval vein were freed from ligamentous attachments, then the main phrenic vein and right adrenal vein were ligated with 6-0 silk sutures and opened using an electric knife. A 24-gauge cannula was inserted into the pyloric branch of the portal vein, with the tip in the portal lumen. The right renal vein was ligated using 6-0 silk sutures and the same cannula was inserted *via* the vein into the inferior *vena cava* until the tip lay near the caudal side of the liver. The distal part of the portal vein, suprahepatic and distal part of the inferior *vena cava* were clamped to isolate the hepatic circulation. Portal pressure was determined by inserting a micro pressure probe together with the cannula into the portal vein.

The perfusion system consisted of a peristaltic pump (Gilson, Inc., Middleton, WI, U.S.A.), and a perfusion circuit with the syringes filled with perfusate. For the basic perfusate, we used lactate-Ringer solution (LRS) containing heparin (3000 IU/l) as an anticoagulant. The perfusion procedure consisted of three sequential steps: preperfusion (10 ml) for flushing out the blood components; perfusion (10 ml) for delivering the vectors, and postperfusion (10 ml) for washing out the excess vectors. Flow rate was calibrated before each perfusion experiment.

After the perfusion, all the clamped vessels were released. The pyloric branch and the right renal vein were decannulated and ligated. The intestines were warmed to 37 °C, and the abdomen was closed using standard procedures. After surgery, each rat was allowed to recover in a warmed cage with free access to water.

Detection of EGFP Activity Four rats were killed 12 h after the administration of SeV-EGFP (10^8 pfu) by hepatic perfusion. The liver was fixed *in situ* by perfusing with 4% paraformaldehyde in phosphate buffered saline (PBS) (pH 7.4) and then divided into 5 mm-thick cubes. These were incubated in 5% to 30% sucrose in PBS, flash frozen in O.C.T. compound (Miles Inc., Elkhart, Indiana, U.S.A.) and sectioned (5 μm) using a cryostat. EGFP was detected under fluorescence microscopy using a GFPA optical filter cube (Olympus, Tokyo, Japan). For histological examinations, tissue sections were stained with hematoxylin and eosin.

Determination of Firefly Luciferase Activity Rats were killed 4 h after the administration of SeV-luc (10^8 pfu) by hepatic perfusion, and the liver, lungs, heart, left kidney, spleen, thymus and testes were removed. Luciferase activities in each tissue were determined as described,[26] except that the samples were first homogenized using a microhomogenizer (Nichion, Chiba, Japan) in lysis solution containing protease inhibitors (10 μg/ml each of E-64, aprotinin, leupeptin and pepstatin A, and 0.5 mM phenylmethylsulfonylfluoride) and the homogenates were clarified by brief centrifugation (1000 ***g*** for 10 min). Protein was determined using a BCA protein assay kit (Pierce, Rockford, U.S.A.).

RESULTS

The physical size of the gene transfer vectors is one of the critical parameters determining their accessibility to the parenchymal hepatocytes *in vivo*. Viral vectors successfully used for delivering genes into the hepatocyte (adenovirus, lentivirus and adeno-associated virus vectors), have the sizes (30—90 nm in diameter) well below the inner diameter of the mesh of the hepatic sinusoids (*ca.* 100 nm). However, the Sendai virus particle is much larger, with a diameter of over 200 nm. Furthermore, Sendai viruses show extensive heterogeneity in size, with diameters ranging from 160 to 600 nm, depending on the number of RNA genomes encapsulated in a single particle.[27] Therefore, selecting and using homogenous Sendai virus particles is a key factor for evaluating delivery through the hepatic sinusoid.

To obtain a homogenous virus preparation, we purified viral particles on gel filtration using Sephacryl S1000,[22] and the sizes of the purified particles in each fraction were determined by dynamic light scattering. As shown in Figs. 1a and b, the viral particles recovered in major peak fractions on gel filtration were acceptably homogenous in size (235 5 nm in diameter, with a polydispersity index below 0.1). The purified virus suspensions were frozen in small aliquots in the presence of dimethyl sulfoxide, and were thawed just before use. This freezing and thawing did not alter the infectivity or